Bird, D. E., Hall, S. A., Casey, J. F., and Millegan, P. S., 1999, Tectonic evolution of the Grenada Basin: *in*, Mann, P. (editor), *Caribbean Basins: Sedimentary Basins of the World*: Hsu, K. J. (series editor), Elsevier Science B. V., v. 4, p. 389-416.

Chapter 15

Tectonic Evolution of the Grenada Basin

DALE E. BIRD, STUART A. HALL, JOHN F. CASEY and PATRICK S. MILLEGAN

Detailed analyses of gravity, seismic reflection and refraction data are integrated with an earlier interpretation of magnetic data to produce a coherent model for the tectonic evolution of the Grenada basin that suggests that the basin formed by near east–west extension.

Although the seafloor of the Grenada basin changes from smooth and undisturbed in the south to rugged with relatively high relief in the north, Bouguer anomalies and two-dimensional and three-dimensional gravity models, based upon seismic refraction and reflection data, reveal that the crust gradually thins in an east–west sense towards the center of the basin. Typical back-arc crust is observed in the southern part of the basin, but refraction data are not sufficiently reliable in the northern part to adequately determine the nature of the crust.

Several curvilinear discontinuities in magnetic, gravity and bathymetric trends are observed. These discontinuities, when integrated with two-dimensional and three-dimensional modeling and analyses of Bouguer gravity anomalies, are interpreted to be due to late Tertiary compressional forces in the northern part of the region. These compressional forces have resulted in the bifurcation of the Lesser Antilles island arc north of 15°N, the westward displacement of part of the Aves Ridge (a remnant island arc), and the crustal deformation observed in the northern Grenada basin. The compressional forces also appear to have sufficiently disrupted the crust in the northern Grenada basin such that earlier magnetic anomaly patterns have been modified to yield the observed magnetic signature.

INTRODUCTION

Various orientations ranging from north–south to east–west have been proposed for the direction of extension and subsequent formation of the Grenada basin (Tomblin, 1975; Bouysse, 1988; Pindell and Barrett, 1990). Large-amplitude, long-wavelength magnetic anomalies, oriented generally east–west over the basin, have been used by authors to arrive at these conflicting interpretations of the basin's evolution.

The Grenada back-arc basin (Fig. 1) formed in early Tertiary time at approximately 12°N (Duncan and Hargraves, 1984; Ghosh et al., 1984; Pindell et al., 1988; Ross and Scotese, 1988). Anomalies produced by east–west-trending features at low magnetic latitudes have significantly larger amplitudes than anomalies produced by north–south-trending features. The orientation of the Earth's magnetic field at low latitudes is nearly horizontal and its direction is essentially to the north, therefore east–west-oriented features produce large perturbations in the Earth's magnetic field while north–south-oriented features result in minor anomalies. If the Grenada basin formed by east–west extension, then magnetic anomalies produced by east–west seafloor spreading in the back-arc region would be characterized by small amplitudes. Furthermore, if these north–south spreading centers were offset by east–west-trending features, then anomalies produced by these features would exhibit large amplitudes that would overwhelm the north–south-trending anomalies.

We have previously analyzed shiptrack and gridded magnetic data over the Grenada basin, including anomaly trend analyses and three-dimensional forward modeling (Bird et al., 1993). Subtle, subparallel to the Lesser Antilles island arc anomalies have been identified over the southern part of the basin and are interpreted to be due to near east–west extension. Amplitudes of these anomalies are approximately 40 nT while amplitudes of east–west-oriented anomalies are about 300 nT. This seven-fold increase, the difference between north–south- and east–west-oriented profiles, was further supported by three-dimensional forward modeling.

Although results from our analyses of magnetic data support near east–west extension, and probable

Caribbean Basins. Sedimentary Basins of the World, 4 edited by P. Mann (Series Editor: K.J. Hsü), pp. 389–416.

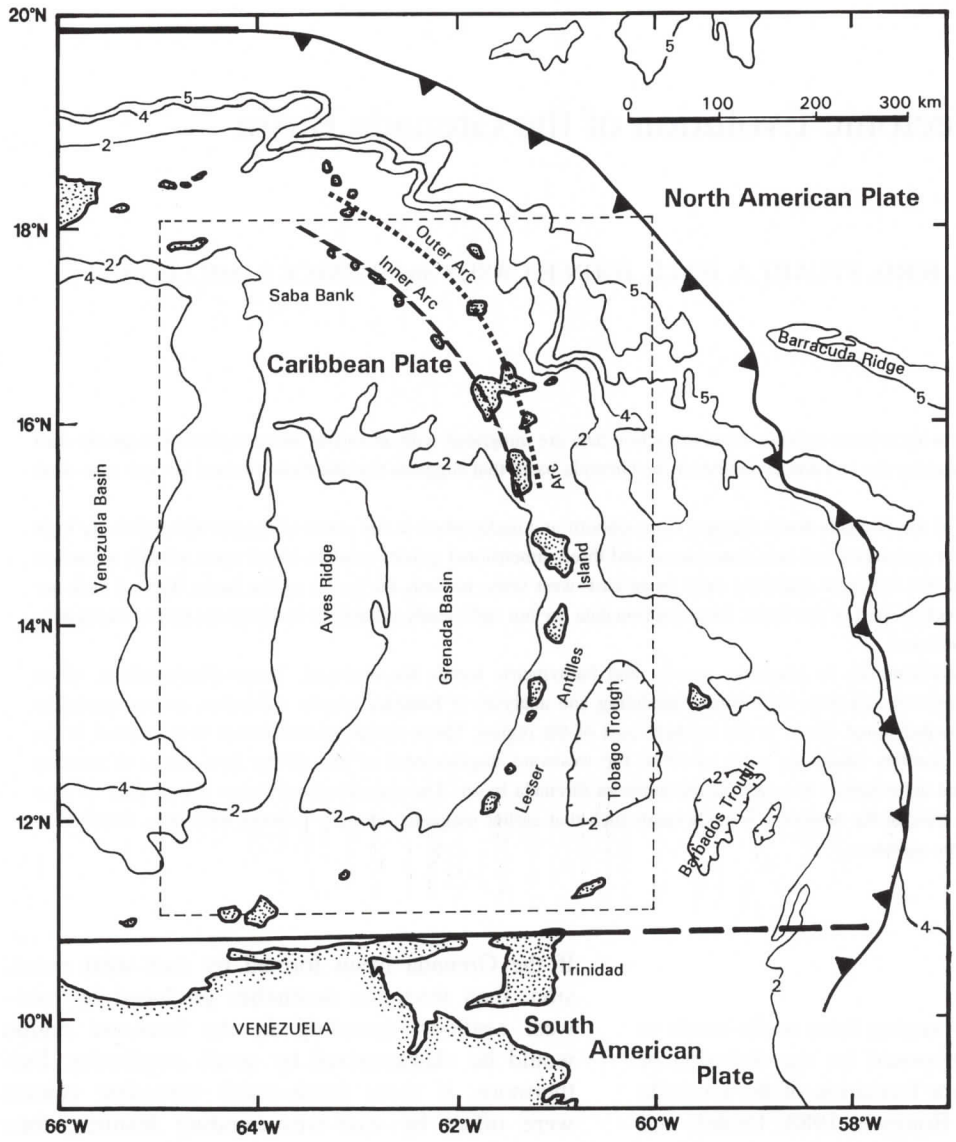

Fig. 1. Physiography of the eastern Caribbean with 2, 4 and 5 km isobaths contoured (after Bouysse, 1984). The outline of the study area, trace of the subduction zone, and strike-slip fault zones which define the North American/Caribbean and South American/Caribbean plate boundaries are displayed. Heavy dashed lines indicate probable locations for plate boundaries. The inner and outer arcs are represented by dashed and dotted lines, respectively.

back-arc spreading for the formation of the Grenada basin, the results should be integrated with analyses of gravity and seismic data to provide more evidence with which to examine the evolution of the region. In this study, interpretations of seismic and gravity data are combined with our earlier interpretation of magnetic data. Then two-dimensional and three-dimensional forward models, incorporating gravity and seismic data (both reflection and refraction), are constructed for the region. Comparison of these results for the Grenada basin with the morphology of the younger Andaman Sea back-arc basin (11 Ma) provide a compelling interpretation for the evolution of the Grenada basin (Mukhopadhyay, 1984).

MODELS FOR THE FORMATION OF THE GRENADA BASIN

Various kinematic models for the formation of the Grenada basin are described by Tomblin (1975), Bouysse (1988), Pindell and Barrett (1990) and Bird et al. (1993). These models outline the formation of the basin by near east–west, northeast–southwest extension, north–south extension and east–west extension, respectively.

East–west extension

Tomblin (1975) describes two possible scenarios for east–west extension. The first involves an early

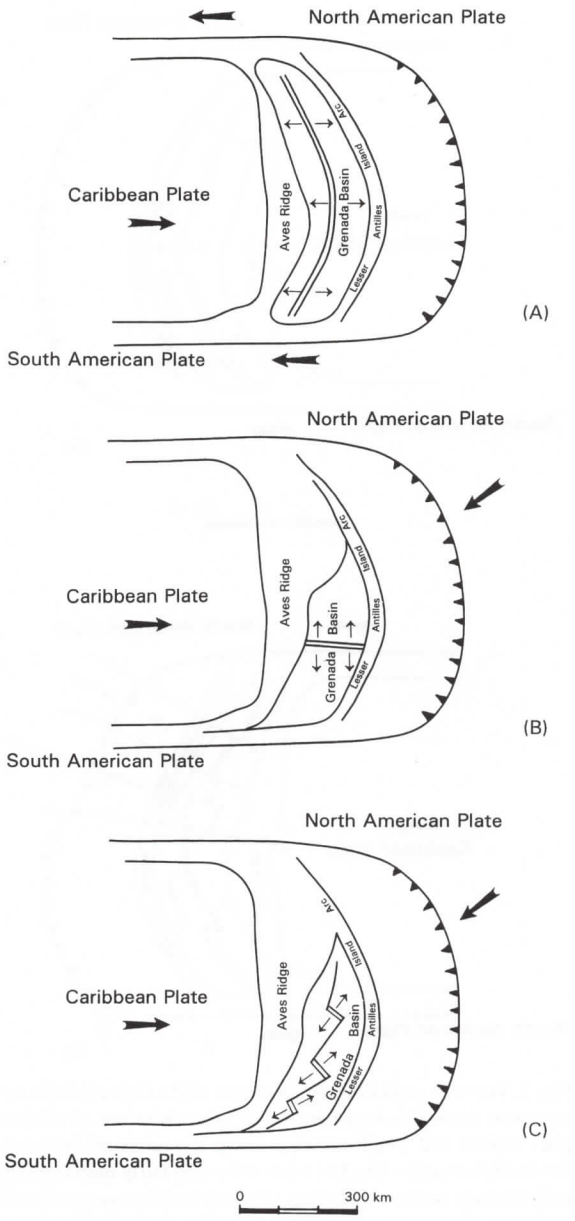

Fig. 2. (A) Possible east–west extension due to a westward shift of the Aves Ridge for the opening of the Grenada basin (Tomblin, 1975). (B) Possible north–south extension for the opening of the basin (Pindell and Barrett, 1990). (C) Possible northeast–southwest extension for the opening of the basin (Bouysse, 1988). Large arrows indicate the relative motions of the North American, Caribbean, and South American plates and small arrows indicate the directions of extension for the formation of the basin.

Tertiary eastward shift of the subduction zone, and the second involves a westward shift of the Aves Swell (Fig. 2A). In the first model the older rocks of la Désirade would either have been part of an older orogeny and moved eastward with the subduction zone, or they may represent obduction of part of the Atlantic floor onto the eastward moving Caribbean plate. Tomblin's alternative scenario for the formation of the basin (a shift of the Aves Ridge to the west) requires the formation and subsequent spreading from a north–south-oriented median ridge. He reports that no such ridge is observed. However, since extension is no longer evident in the Grenada basin, the loss of heat at spreading centers would cause the ridge system to cool and subside. Therefore a ridge system may not be obvious in the data, but the center of the basin would still produce a Bouguer gravity high when compared to thicker crust on either side. Intuitively, east–west extension as proposed by Tomblin seems most reasonable, and magnetic anomaly lineations over many back-arc basins support this conclusion (i.e., the South Sandwich, Lau, Havre, North Fiji, Banda Sea, Parece-Vela, Shikoku, and Sea of Japan basins).

North–south extension

Pindell and Barrett (1990) feel that the Leeward Antilles were coupled to the northern edge of the South American plate and that north–south spreading in the Grenada basin is a result of continued eastward progression of the Caribbean plate. The basin therefore formed by right lateral shear (Fig. 2B). In this model the Leeward Antilles may have been part of the Aves Ridge prior to the formation of the basin and represents fragmentation of the arc as the Caribbean plate progressed eastward. If the long-wavelength, high-amplitude, east–west-trending magnetic anomalies over the basin are produced by seafloor spreading, then this model appears to fit the magnetic data.

For this model differences in the nature of the crust between the northern and southern parts of the basin are important. Pindell and Barrett (1990) suggest that the northern part of the basin is block faulted with no development of oceanic crust; however, the southern part of the basin may be underlain by oceanic crust. Although Pindell and Barrett's model may appear overly complex, magnetic anomaly patterns over the Andaman Sea basin appear to be oriented at a high angle to the trench line of its subduction zone.

Northeast–southwest extension

Similar to Pindell and Barrett's model, Bouysse (1988) describes a possible mechanism for extension in which coupling of the southern part of the Lesser Antilles with the South American plate precedes the opening of the basin (Fig. 2C). He suggests that the Netherlands-Antilles, Lesser Antilles and Greater Antilles formed a continuous Mesozoic arc prior to the injection of the Caribbean plate between the American plates. Bouysse further theorizes that subsequent seafloor spreading was oriented northeast–southwest at the onset of the Cenozoic in a seg-

mented manner such as described by Tamaki (1985) for the Sea of Japan basin. Initial spreading was in the southernmost portion of the basin and gradually progressed northward over time.

Bouysse's model provides for contemporaneous formation of the Yucatan and Grenada basins. This development occurred when the northeast-travelling Caribbean plate, with respect to the North American plate, was wedged between the North American and South American plates in Late Cretaceous/early Tertiary time. Subsequent to this collision, the Caribbean plate rotated clockwise and began travelling in an east–west direction.

Near east–west extension

Bird et al. (1993) interpret the basin to have formed by near east–west extension similar to that described by Tomblin (1975) with late Tertiary tectonic movements disrupting the crust, and magnetic signature, over the northern part of the basin (Fig. 3). These conclusions are supported by forward three-dimensional magnetics modeling and identification of subtle anomaly trends over the southern part of the basin. These low-amplitude (about 40 nT) anomalies are interpreted as those produced by a roughly north–south-oriented spreading center(s) near the geomagnetic equator. The chaotic, patchy anomalies over the northern part of the basin are thought to have formed by seafloor spreading also, but later were disrupted by the late Tertiary event responsible for the bifurcation of the Lesser Antilles.

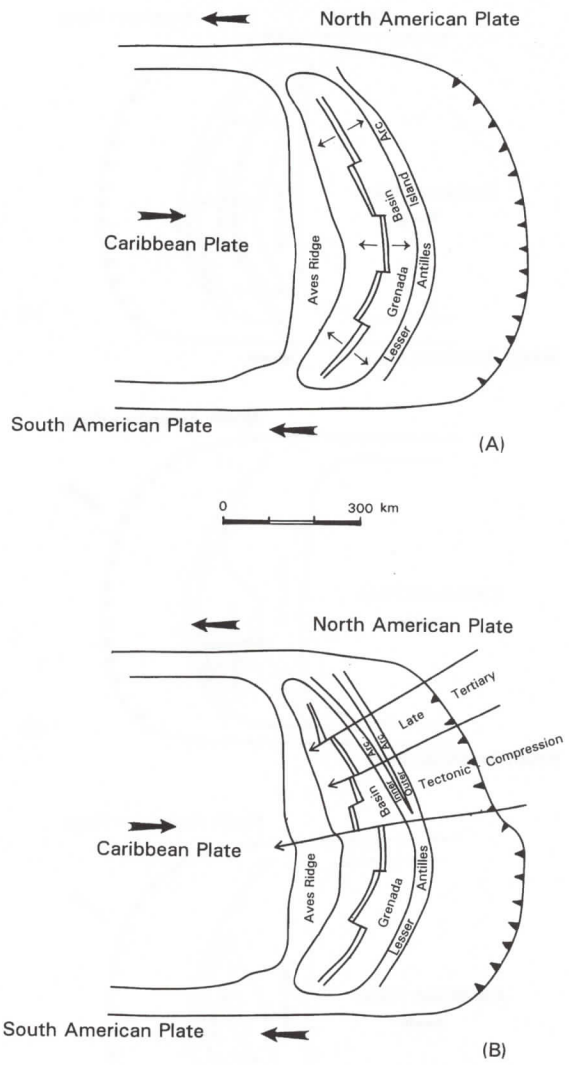

Fig. 3. Two-step model for the formation of the Grenada basin by east–west extension. Large arrows indicate directions of relative plate motion and small arrows indicate directions of extension and basin formation. (A) The basin is formed fairly uniformly by early Tertiary seafloor spreading. (B) Late Tertiary compressional tectonism disrupts the northern part of the basin (indicated by long northeast-oriented arrows).

DATA BASE

The data base for this study includes gridded gravity and bathymetry data (Figs. 4 and 5, and Web-Figs. 15.1–4[1]), shipboard gravity and bathymetry profile data (Fig. 6), multiple channel seismic reflection sections (Fig. 7A), and reversed and unreversed seismic refraction profiles (Fig. 7B). Grids of total intensity magnetic anomalies (2 km) and free-air gravity (6 km) were compiled in 1987 by the Geological Society of America Decade of North American Geology (DNAG) Committees on the Magnetics and Gravity Maps of North America, respectively. These grids are available from the NOAA/National Geophysical Data Center (NGDC). The bathymetry grid is a portion of the ETOPO5 data. The ETOPO5 data set is a 5-minute grid of topography and bathymetry for the entire world and is available from the NGDC as well. Since the grid spacing is not constant as latitude varies, the data were regridded to 9 km utilizing a moving average least squares method.

[1] Available at http://www.elsevier.nl/locate/caribas

Multi-channel seismic reflection lines were obtained from the Institute Français du Petrole (IFP), Lamont-Doherty Geological Observatory (LDGO) of Columbia University, and the University of Texas at Austin (UT) Institute for Geophysics (Fig. 8). The reflection lines obtained from UT were originally acquired by Gulf Oil Company (GULFREX lines). Identification, fold, orientation, length, and year of acquisition of seismic reflection sections used are displayed in Table 1. Seismic reflection line RC1904 (LDGO) was available in digital form as well as its corresponding velocity analyses. Nine horizons of this line were analyzed by LDGO and those within the basin were used to interpret a velocity function for modeling.

Refraction information used for the study comes

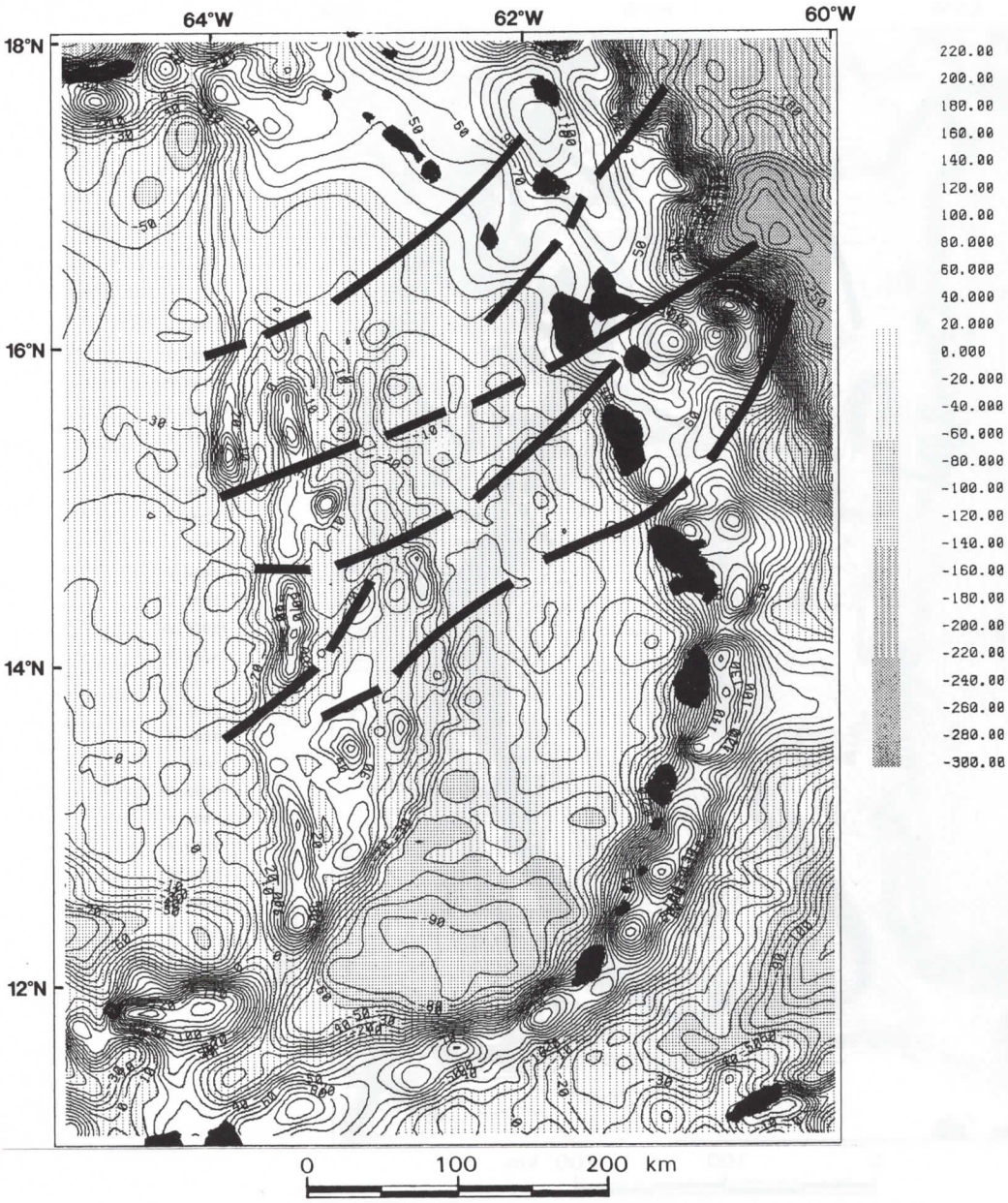

Fig. 4. Free-air gravity anomalies over the study area. Heavy solid and dashed lines indicate interpreted curvilinear zones of disruption (dashed lines indicate reduced confidence). Contour interval is 10 mGal.

Table 1

Parameters of multiple channel reflection seismic data

Organization	Line No.	Fold	Direction	Year	Length (km)
LDGO	C1904	24	E	1975	870.50
IFP	A4	48	SE	1973	116.66
IFP	118A	48	E	1974	169.77
IFP	131A	48	SE	1974	222.73
IFP	217A	48	N	1976	111.36
UT (GULFREX)	LS-11	48	NE	1975	169.85
UT (GULFREX)	LS-12	48	NE	1975	143.96
UT (GULFREX)	LS-14	24	E	1975	304.84
UT (GULFREX)	LS-15A	24	NE	1975	165.40
UT (GULFREX)	VB-11	24	NE	1975	138.73
UT (GULFREX)	VB-12	24	SE	1975	132.89
Total					2546.69

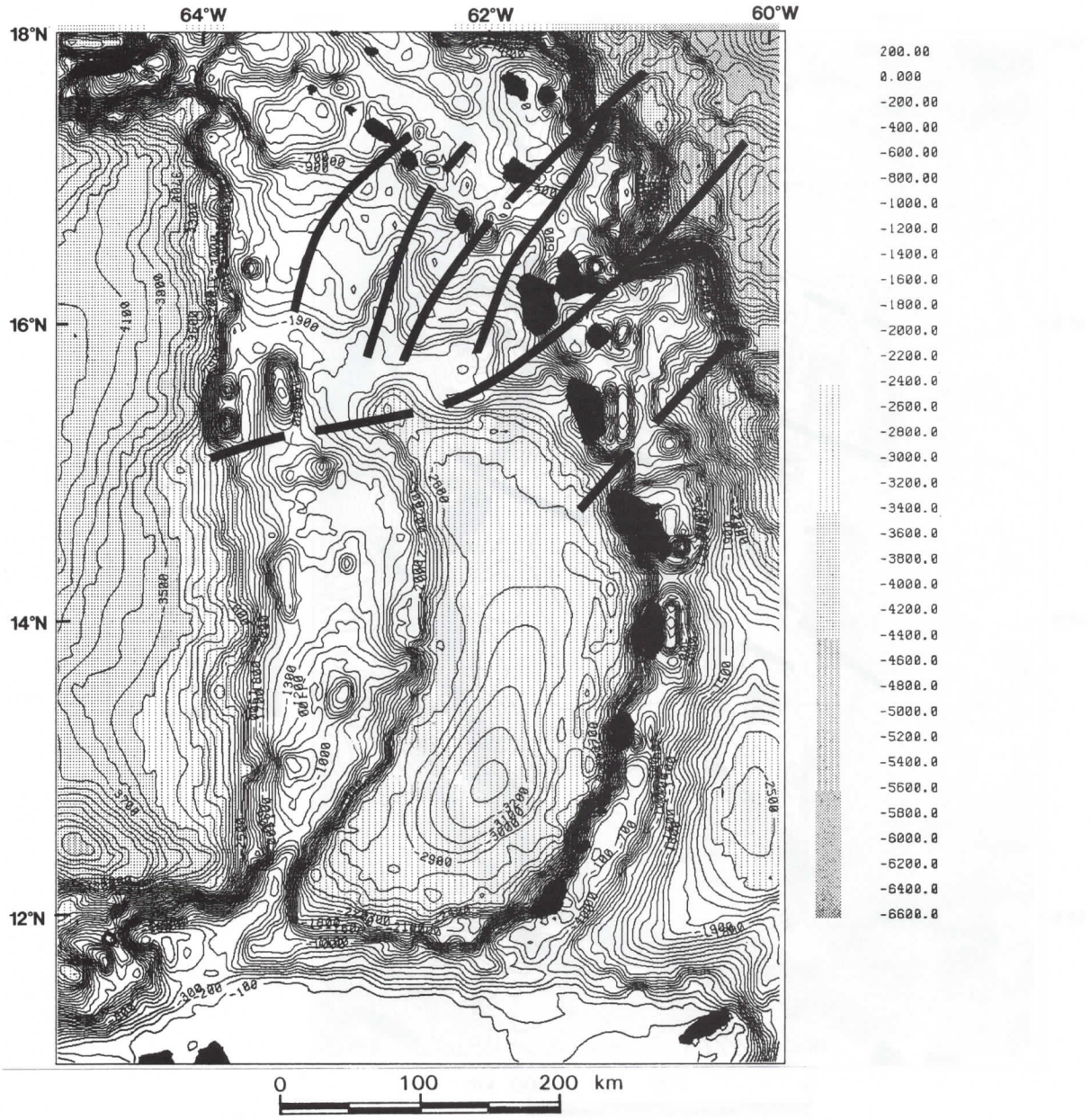

Fig. 5. Bathymetry of the study area. Heavy solid and dashed lines indicate interpreted curvilinear zones of disruption (dashed lines also indicate reduced confidence). Contour interval is 100 m.

from published studies (Ewing et al., 1957; Officer et al., 1959; Edgar, 1968; Boynton et al., 1979; Speed and Westbrook, 1984). In general, coverage of refraction data is sparse, particularly in the northern part of the basin where the velocity structure is represented by a single, unreversed profile (Fig. 7B).

TECTONICS OF BACK-ARC BASINS

Models for the formation of back-arc basins are discussed by, among others, Karig (1971), Sleep and Toskoz (1971), Poehls (1978), Uyeda and Kanamori (1979), Dewey (1980), Cross and Pilger (1982), Taylor and Karner (1983), and Tamaki (1985). A back-arc basin is defined here as an extensional basin located at the edge of an overriding plate of a subduction zone such that the basin formed after initiation of subduction.

At least nineteen basins have formed around the world by extension, or seafloor spreading, behind island arcs (Table 2). Back-arc basins formed by organized seafloor spreading should produce magnetic anomalies parallel to spreading centers and those with well defined magnetic anomaly lineations include the South Sandwich, Shikoku, Bismark, South Fiji, Lau, Havre, Banda, and Andaman basins (Taylor, 1979; Weissel, 1980, 1981; Barker and Hill, 1981;

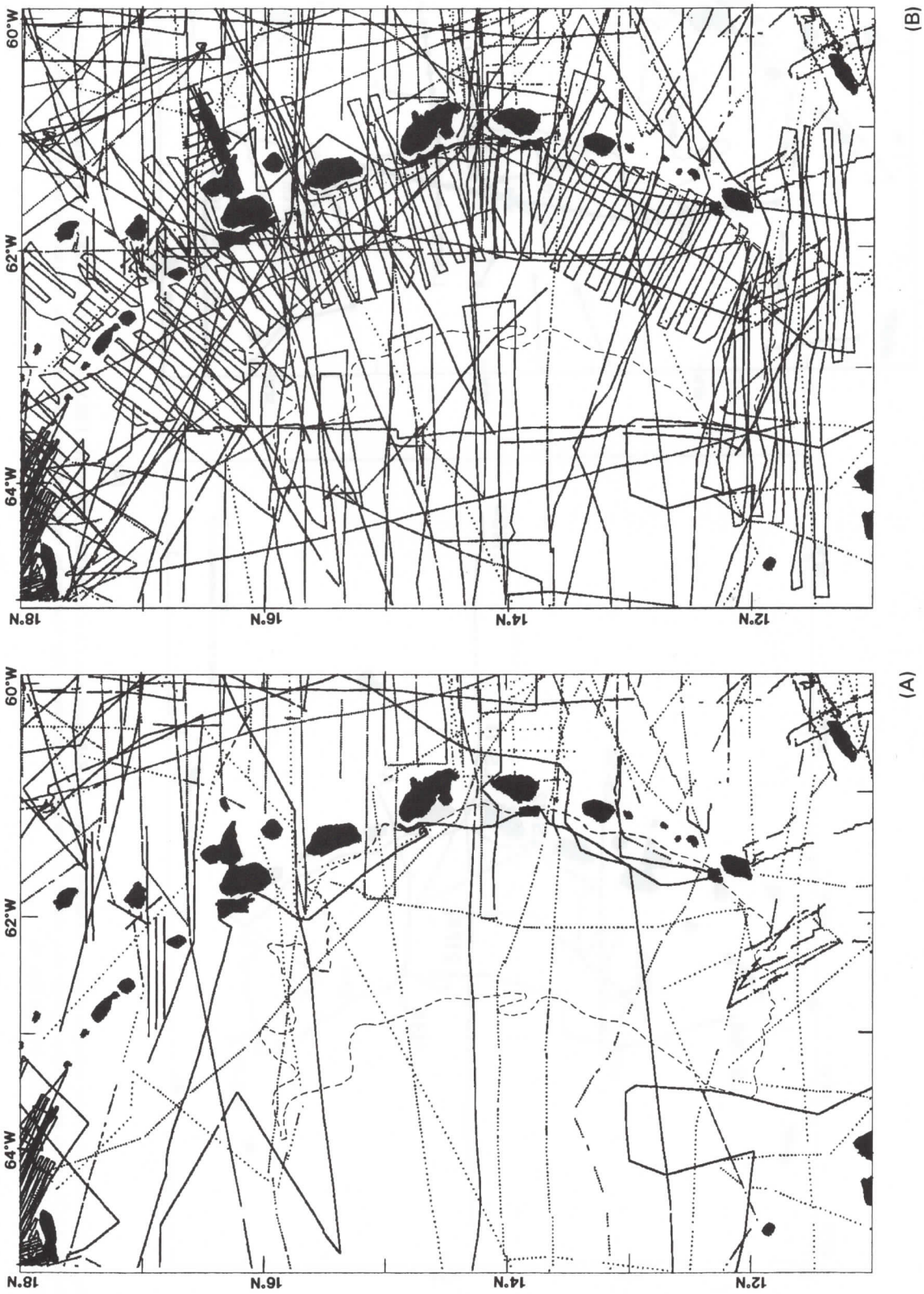

Fig. 6. Shiptrack data coverage in the study area: (A) gravity, (B) bathymetry.

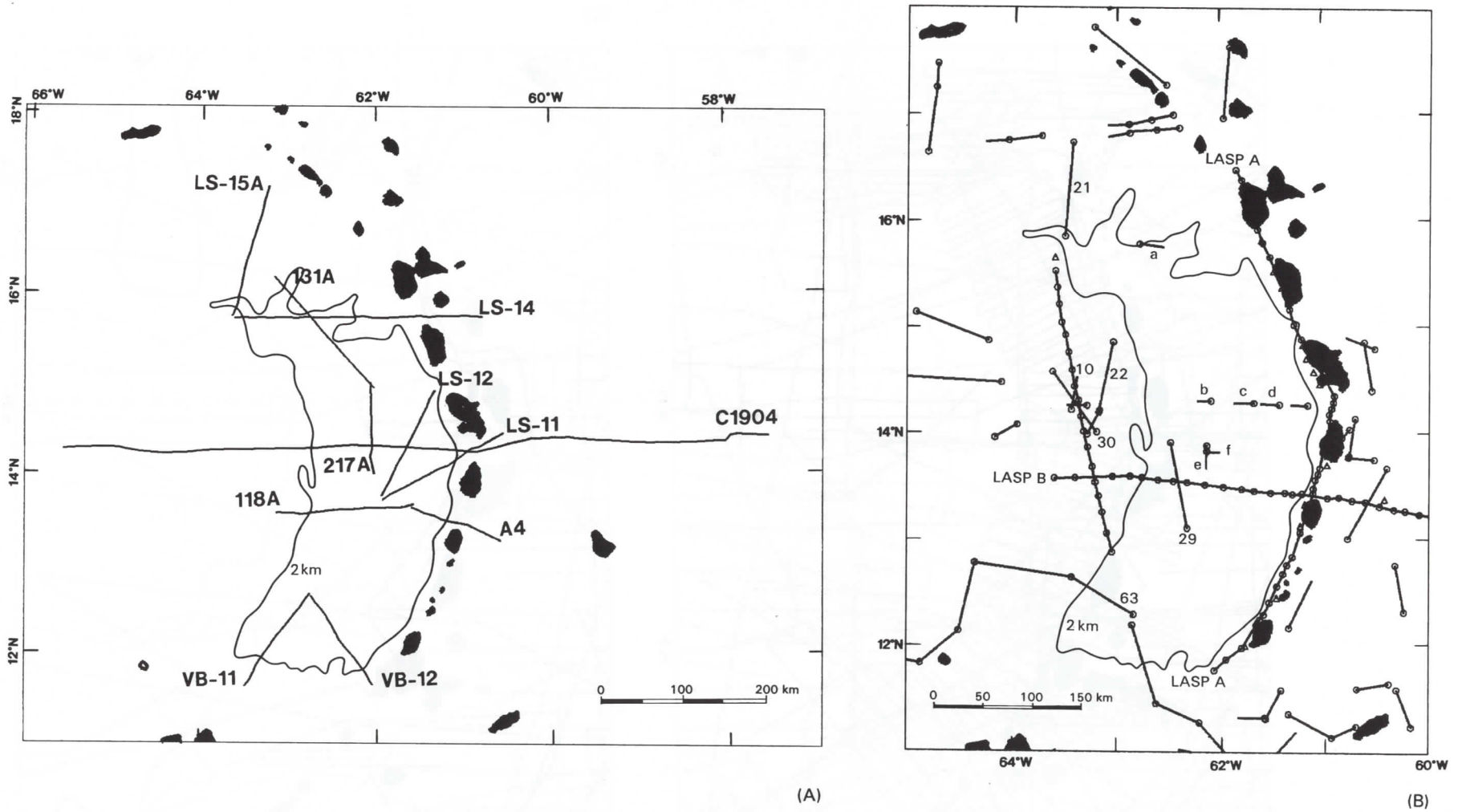

Fig. 7. Multi-channel seismic reflection data and refraction profiles. (A) Reflection data. *LS* = GULFREX, *VB* = GULFREX, *A* = IFP, *C* = LDGO. (B) Refraction data. For the Lesser Antilles Seismic Project (*LASP*), circles and triangles indicate shot and receiver locations, respectively, otherwise circles indicate receiver locations for the reversed and unreversed profiles. Velocities for profiles LASP B, 21, 22, 29, a, b, c, d, e, and f are shown in Fig. 15.

Table 2
Back-arc basins of the world

Basin	Subduction zone
Aegean	Hellenic
Andaman	Andaman
Banda	Java
Bismark	New Britian
Fiji Plateau	New Hebrides
Grenada	Lesser Antilles
Havre	Kermadec
Kurile	Kurile
Lau	Tonga
Mariana	Mariana
Okinawa	Ryuku
Parece-Vela	Mariana
Sea of Japan	Japan
Shikoku	Bonin
South Aleutian	Aleutian
South Fiji	Kermadec, Tonga
South Sandwich	South Sandwich
Tyrrhenian	Hellenic
Yucatan	Cuban

Bandy and Hilde, 1983; Brooks et al., 1984; McCabe et al., 1985, 1986). Some back-arc basins have anomaly patterns characterized by weak or subtle trends including the Grenada, Sea of Japan, Parece-Vela, and West Fiji basins (Weissel, 1981; Brooks et al., 1984; Speed and Westbrook, 1984; Tamaki, 1985; Bird et al., 1993). Finally, some back-arc basins have no predominant magnetic pattern over them such as the Kurile, Okinawa, and Mariana basins (Lee et al., 1980; Weissel, 1981; Brooks et al., 1984; Okuma et al., 1990). Magnetic anomaly patterns produced by back-arc spreading may be related to the orientations of back-arc extension, which in turn may be related to the interactions between overriding plates and their respective subducting slabs.

Four scenarios that lead to a lack of coherent magnetic lineations over back-arc basins are: (1) complex rifting and segmentation of spreading centers producing incoherent anomaly trends (Tamaki, 1985); (2) young basins, such as the Mariana and Okinawa, not sufficiently developed to produce well defined trends; (3) basins formed by east–west extension near the magnetic equator (the Grenada basin is a probable candidate for this scenario); and (4) a basin formed during a time when there were no geomagnetic reversals, such as in Mid-Cretaceous time (about 118–84 Ma).

Refraction data from the Andaman, Banda, Celebes, Grenada, Havre, Mariana, Okinawa, Parece-Vela, Sea of Japan, Shikoku, and Sulu basins reveal that the crustal structure of back-arc basins is similar to 'typical' oceanic crust described by Ludwig et al. (1971). The nature of back-arc basin crust, however, is more variable. Six back-arc basins, Grenada, Mariana, Okinawa, Parece-Vela, Sea of Japan, and Sulu basins (Ewing et al., 1957; Karig, 1971; Hayes et al., 1978; Bibee et al., 1980; Hussong and Uyeda, 1981; Curray et al., 1979), appear to contain an additional layer exhibiting intermediate velocities between layer 3 and mantle velocities (defined as the transitional layer for this study).

Table 3
Means and standard deviations for the velocity structure of selected back-arc basins (regarding transition layers, means and standard deviations are only calculated for the total of all transition layers)

Back-arc basin	Layer 2		Layer 3		Transition	Mantle	
	M	STD	M	STD		M	STD
Sea of Japan	5.5	0.2	6.4	0.4	7.4, 7.5	8.0	0.2
Okinawa	5.1	0.3	6.0	0.2	7.1, 7.4	–	–
Shikoku	4.9	0.6	6.7	0.3	–	8.2	0.3
Parece-Vela	5.3	0.5	6.9	0.1	7.7	8.4	0.2
Andaman	5.4	0.3	6.2	0.3	–	–	–
Sulu	5.4	0.3	6.4	0.3	7.2	8.3	–
Celebes	5.2	0.2	6.7	0.3	–	8.1	0.3
Banda	5.1	–	6.6	–	–	8.0	–
Grenada	4.9	0.5	6.2	0.2	7.4, 7.4	8.2	–
Mariana	5.1	0.6	6.2	0.4	7.2, 7.4	8.2	0.4
Havre	4.4	–	6.6	–	–	8.5	–
Means	5.1	0.3	6.4	0.3	7.3, 0.2	8.2	0.2

Table 3 displays results from the eleven back-arc basins studied by analyses of refraction velocities. Means and standard deviations of the data are displayed for each basin as well as for the entire data set. The standard deviations illustrate the variability of the data, while the means support the concept of layered crusts, similar to normal oceanic.

REGIONAL SETTING

Geology

The Grenada basin is bounded to the north by the Saba Bank at the junction of the Greater and Lesser Antilles, and to the south by the continental rise of northern Venezuela (Fig. 1). The Aves Swell (or Ridge) and the Lesser Antilles arc form the western and eastern limits of the basin, respectively. The shape of the basin is arcuate with approximate dimensions of 640 km (north–south) by 140 km (east–west), its water depth ranges from about 2 to 3 km. Sediment thickness ranges from 2 km in the north to 9 km in the south (Bouysse, 1988). Morphologically, the ocean floor of the Grenada basin can be divided into northern and southern parts at about 15.5°N. The bathymetry of the northern part is rugged while the southern part of the basin is characterized by a near-horizontal, smooth seafloor. The nature of the sediments in the Grenada basin is not known; however, refraction data indicate that

sediments of the Aves Ridge extend and thicken into the basin (Westbrook, 1975).

The Aves Swell, an extinct island arc (Bouysse, 1984, 1988), is oriented north–south and dips steeply into the Venezuela basin to the west. Its eastern edge is arcuate, similar to the Grenada basin, and descends in steps into the Grenada basin. Fox and Heezen (1975) report volcanic rocks consisting of andesites, basalts, dacites and volcanic breccias recovered from pedestals and scarps of the Aves Ridge. They also report Middle Eocene fossiliferous limestones, marls and chert recovered from dredge hauls. Late Cretaceous to Paleocene granodiorites, diabases and basalts, dredged from the southern part of the Aves Ridge, may be part of the Aves Ridge or the northern edge of the South American platform (Fox and Heezen, 1975).

Like the eastern edge of the Aves Swell and the Grenada basin, the general shape of the Lesser Antilles island chain is arcuate. It bifurcates at about 15°N with a maximum separation of about 50 km at its northern limit. The outer arc is older (generally middle and late Paleogene to early Neogene) and inactive, while the inner arc is younger (generally Neogene to Quaternary) and presently active (Fox and Heezen, 1975). The western limit of the arc is marked by steep bathymetric gradients into the Grenada basin. Bouysse (1988) reports two episodes of volcanism: the first in Late Cretaceous time prior to back-arc spreading (84–66.4 Ma), and the second from Eocene to present. Warner (1991) reports that Early Paleocene to Early Oligocene volcanic rocks have been recovered from the Saba Bank. The episodic nature of volcanism is clear because volcanic rocks younger than Early Paleocene to Early Oligocene (Warner, 1991) have not been collected from the Aves Swell and volcanic rocks older than Middle Eocene (with one exception) have not been collected from the Lesser Antilles (Bouysse, 1988). This age difference indicates that the Grenada basin probably formed in early Tertiary time. The duration of back-arc spreading was restricted, as found in other back-arc basins. Jurassic age basalts on the island of la Désirade are thought to represent obducted oceanic crust (Fink, 1968, 1970).

Seismic refraction

The thickness of the crust increases beneath the Aves Ridge and Lesser Antilles and decreases beneath the Grenada basin (Kearey, 1974; Kearey et al., 1975; Westbrook, 1975). Modeling also suggests that the base of the crust generally mirrors the topography and bathymetry (Boynton et al., 1979; Bird, 1991). Oceanic crustal layers 2 (4.9–5.3 km/s) and 3 (6.2–6.4 km/s) are present in the Grenada basin south of about 15°N (Speed and Westbrook, 1984). Boynton et al. (1979) reports that the Grenada basin crust is approximately 14 km thick near 14°N with an average velocity of 4.8 km/s. Descriptions of the velocity structure vary; however, general structure and probable rock types follow: (1) 2.2 and 3.7 km/s — unconsolidated sediments and partially lithified sediments (Boynton et al., 1979); (2) 5.3 km/s — (upper oceanic crust), basaltic flows and dikes (observed only in the southern part of the basin (Speed and Westbrook, 1984); (3) 6.2 km/s — (lower oceanic crust), gabbros; and (4) 7.4 to 7.5 km/s — lower crust to mantle velocity transition zone.

Upper and lower crusts of the Lesser Antilles arc are defined as 6.3 km/s and 6.9 km/s layers totaling about 35 km in thickness (Westbrook, 1975; Boynton et al., 1979). Rocks of the lower crust may be basic in composition while the rocks overlying the upper crust (3.4–4.5 km/s layer) may be composed of limestones, pyroclasts and sediments (Boynton et al., 1979). Officer et al. (1957) describe the seismic structure of the Aves Ridge as similar to that of the Lesser Antilles.

Seismic reflection

Neither of the prominent Caribbean reflectors, A′ or B′, can be traced across the Aves Ridge into the Grenada basin; however "... a lower or middle Miocene horizon can be followed throughout the Grenada basin and west to the crest of the Aves Ridge..." (Speed and Westbrook, 1984). Two outer ridges of the Aves Swell enclose horizontal layers of sediment which are thickest near 13.4°N (Kearey, 1974). Reflection data also suggest that the Aves Ridge continues northward with its topographic expression buried by layers of sediment (Kearey, 1974).

For the purpose of this work, the most important aspect of the seismic reflection data is the character of sediments overlying deep structures in the basin. The rugged bathymetry of the northern part of the basin is produced by deep structures in several locations. Conversely, reflection horizons of the southern part of the basin are smooth and relatively undisturbed (Fig. 7). Sediment thickness increases to the south from approximately 2 to 9 km.

Magnetics

Magnetic anomalies over the Grenada basin (Fig. 9 and Web-Figs. 15.5,6) have been carefully examined by Bird et al. (1993). Anomaly amplitudes of hundreds of nanoteslas and wavelengths ranging from 10 to over 50 km are observed. Anomalies over the southern part of the basin display longer wavelengths and smaller amplitudes than those over

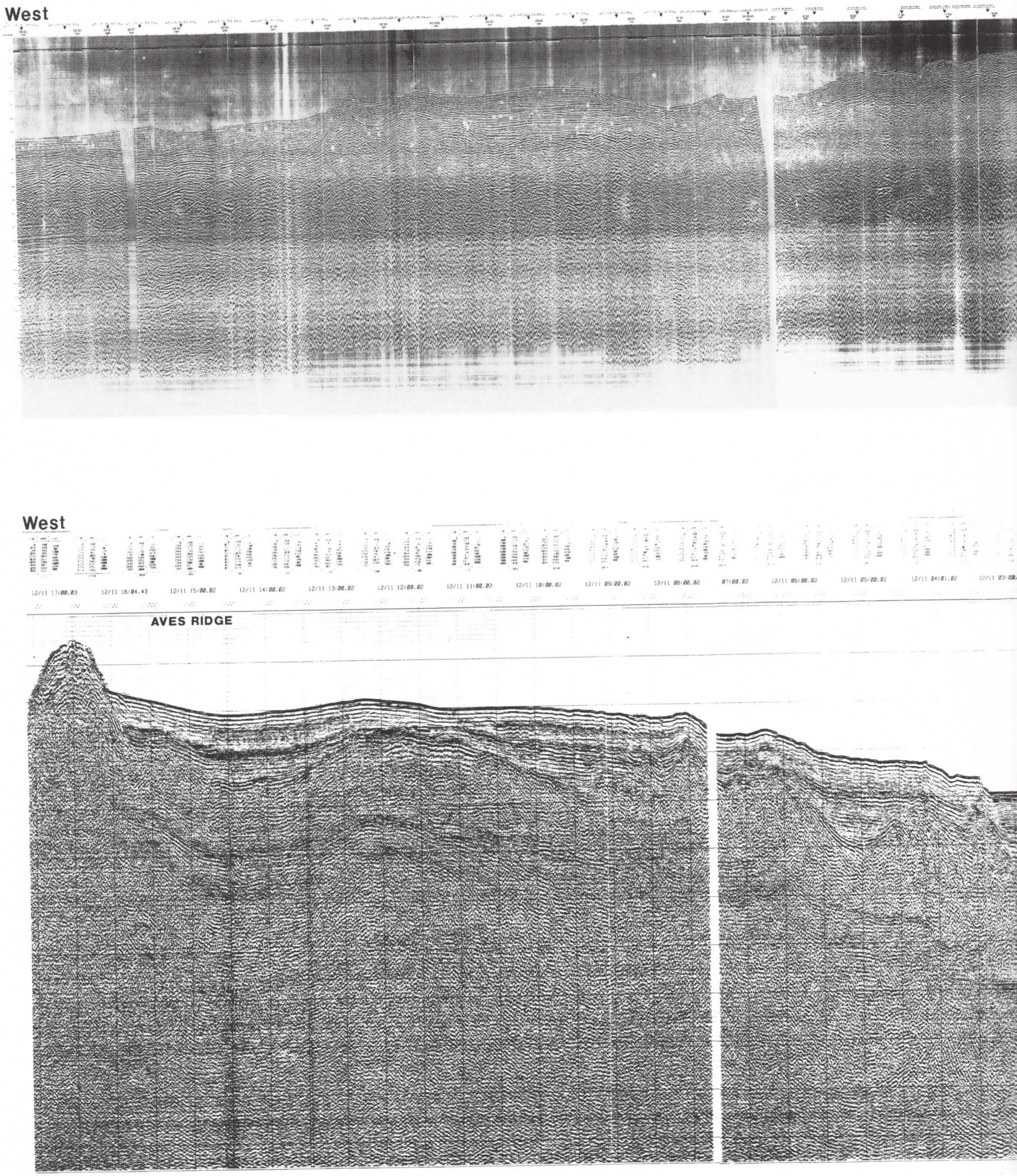

Fig. 8. Part of multiple-channel seismic reflection lines: (A) LS-14; (B) C1904. Locations of these sections are displayed in Fig. 7A.

Line LS-14

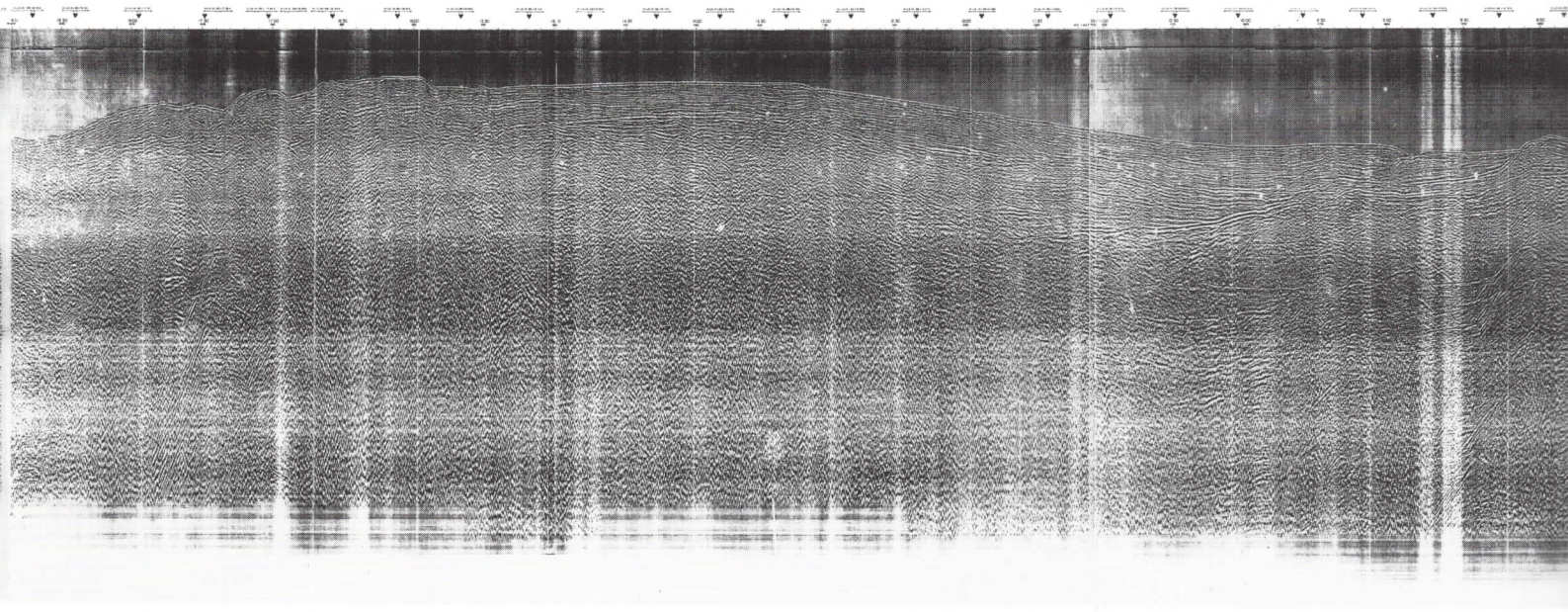

Line C-1904

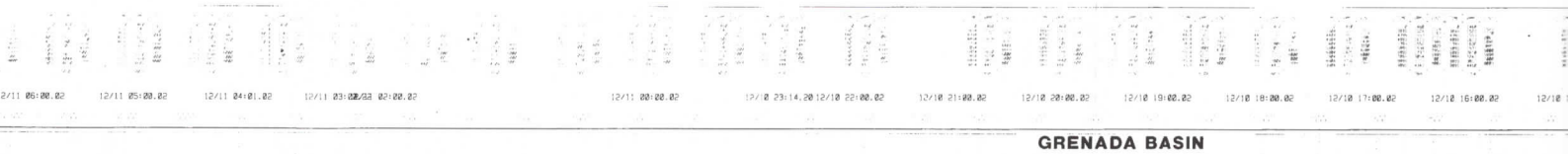

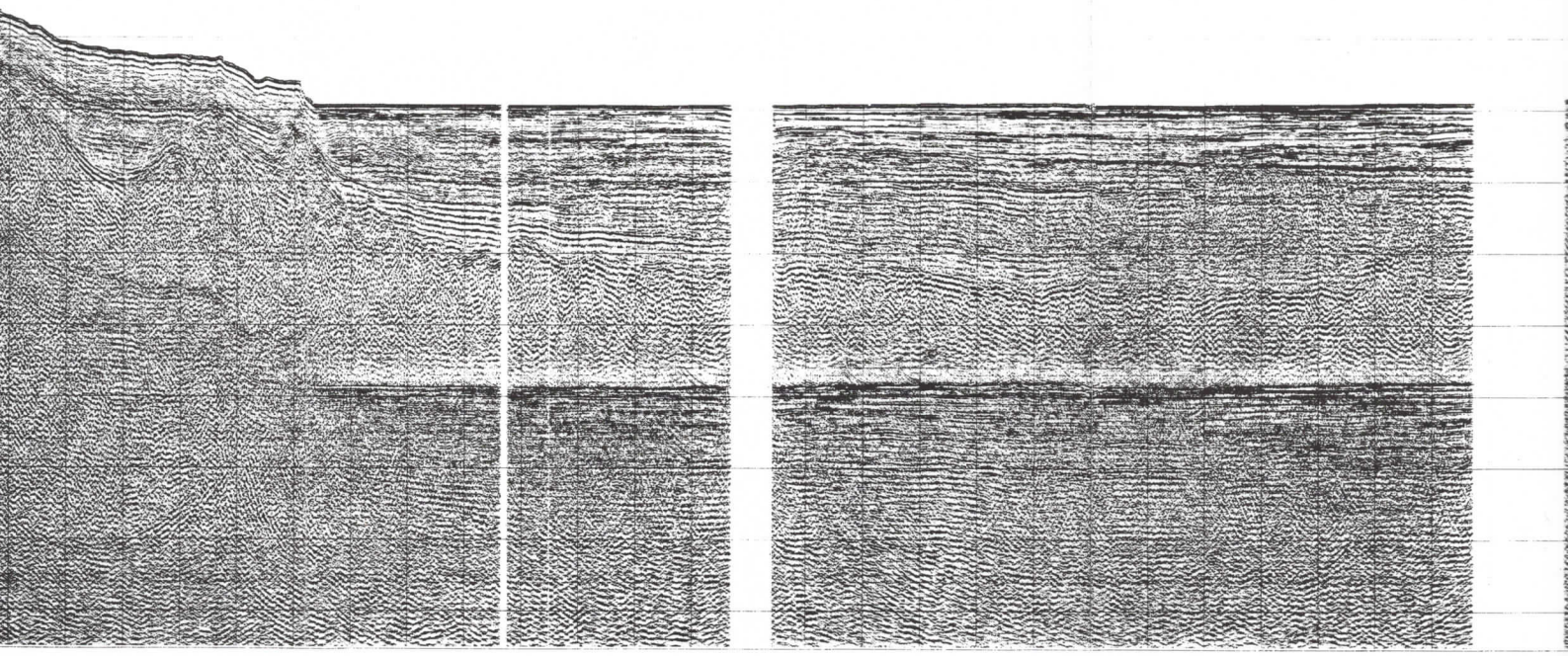

A.

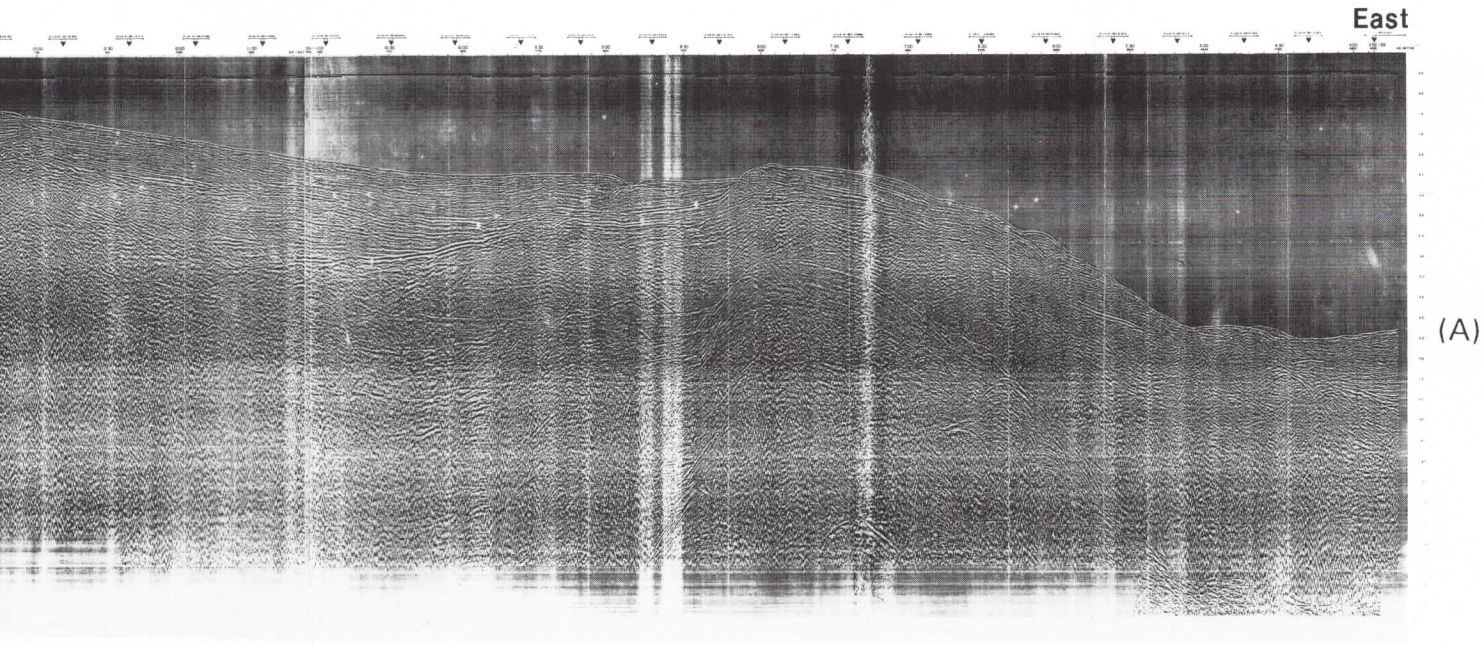

(A)

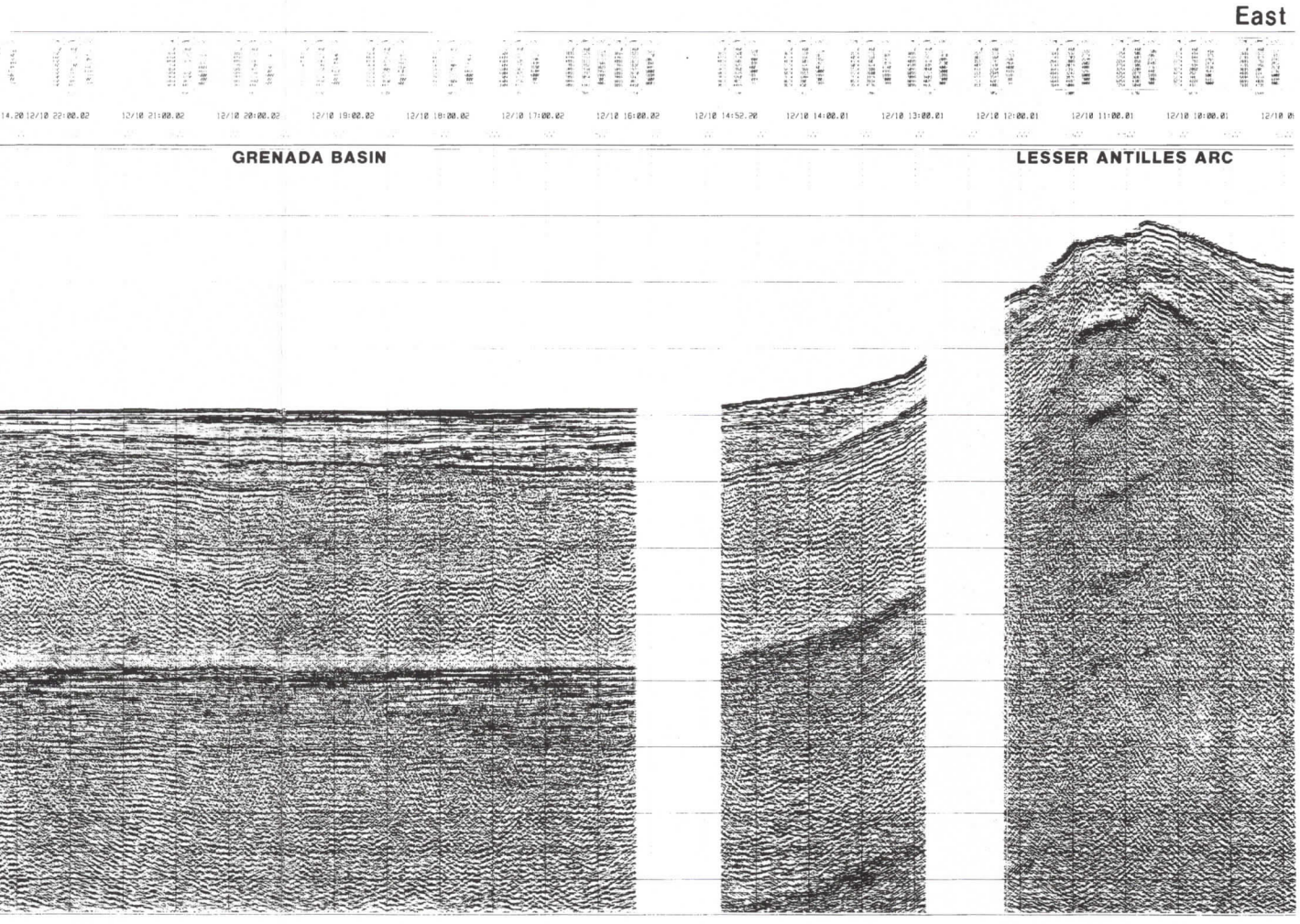

(B)

the northern part. Similarly, shapes and trends of anomalies change from north to south. The shape of the anomalies over the northern part are typically oblong with an east–west trend degrading to patchy and more disorganized farther south. The magnetic anomalies over the Aves Swell are similar to those over the northern part of the basin except that they are oriented north–south with larger amplitudes. The magnetic anomalies over the Lesser Antilles range in amplitude from 150 to 600 nT with wavelengths from 5 to 40 km. Short-wavelength anomalies (20 to 50 km) clearly delineate the island chain.

Gravity

Several high-amplitude (approximately 80 to 150 mGal) free-air gravity anomalies, parallel to and just east of the island arc, are shown in Fig. 4 and Web-Figs. 15.1,2. The wavelengths of these anomalies increase from about 20 km in the south to 50 km in the north. Similarly, several north–south-trending free-air gravity anomalies are observed over the Aves Ridge reflecting bathymetric variations. These anomalies display wavelengths and amplitudes of about 20 km and 50 mGal, respectively. North of the Aves Ridge, the free-air gravity field is subdued, displaying a broad positive northeast gradient (0.6 mGal/km) over the area. The average free-air gravity value ranges from about 0 to −20 mGal over the northern half of the basin, then gradually decreases to about −80 mGal over the southern half.

Airy isostatic reduction was performed by Kearey (1974). Isostatic anomalies over the Aves Ridges are generally negative (−15 mGal) with some positive values to the south. Isostatic anomalies over the Grenada basin decrease from +10 to −30 mGal, north to south. Kearey (1974) calculated 50 mGal positive anomalies over the Lesser Antilles.

INTERPRETATION

The northern part of the Aves Ridge (north of 15°N) appears to be displaced to the west and may be related to the late Tertiary tectonic event which resulted in the westward shift of the Lesser Antilles (Figs. 4 and 5 and Web-Figs. 15.1–4). Therefore, the data are inspected for features which support this hypothesis. Subtle, curvilinear 'discontinuities' are interpreted for total intensity magnetic anomaly, free-air gravity anomaly, and bathymetry data sets. Since these data sets are physically different and related to physically different rock properties, trends are not coincident between the data sets. Discontinuities consist of connected gradients, highs and lows, and/or connected truncations of gradients, highs and lows. Subduction of the aseismic Barracuda Ridge (McCann and Sykes, 1984), or differential motion between the North American and South American plates (Bougault et al., 1988), in the late Tertiary has caused the subducting slab(s) to shoal under the northern part of the overriding Caribbean plate. McCann and Sykes (1984) have further suggested that the Barracuda and Main Ridges are continuous and have been recently overridden by the relative eastward motion of the Caribbean plate. In either case this shoaling has resulted in a westward shift of the center of volcanism beneath the northern part of the Lesser Antilles island arc. In addition to tectonic compression, this shoaling of the subducting slab(s) may have caused sections of the overriding plate (i.e., northern Aves Ridge, Grenada basin, and Lesser Antilles Arc) to be displaced and/or disrupted. Therefore curvilinear discontinuities are interpreted to be related to disruptions within the crust of the basin, which are in turn interpreted to be related to the tectonic event responsible for the bifurcation of the arc.

Gravity

High-amplitude free-air gravity anomalies near the Lesser Antilles arc are interpreted to be produced by a combination of shallow bathymetry as well as dense volcanic rocks. Hence the contrast between the magmatic arc with the surrounding water and sediments results in positive gravity anomalies as seen in the results of 2-D modeling. The long-wavelength low over the southernmost part of the basin is also interpreted to be produced by a combination of effects. Sediment thickness increases to about 10 km, causing the crust to warp down into the mantle. Kearey (1974) reports that negative isostatic anomalies (less than −30 mGal) over the southern part of the Grenada basin may be related to downward flexing of the crust into the mantle.

Bouguer gravity anomalies were calculated in order to compensate for the water bottom interface and allow for the interpretation of crustal variations. Bouguer gravity anomalies were calculated for two cases: (1) substituting rock with a density of 2.0 g/cm^3 for the water layer, and (2) substituting rock with a density of 2.67 g/cm^3 for the water layer (Fig. 10 and Web-Figs. 15.7,8). In both cases a broad high (i.e., positive anomaly) is located over the center of the basin, with a north–south elongation, from about 13°N to 15°N. This high is slightly displaced to the south as the density used to calculate the Bouguer anomalies is increased. A large, triangular-shaped residual low is produced by the Bouguer calculations over the southernmost part of the Grenada basin and adds confidence to the notion that the crust is downwarped into the mantle. In general, the only differences between utilizing a rock

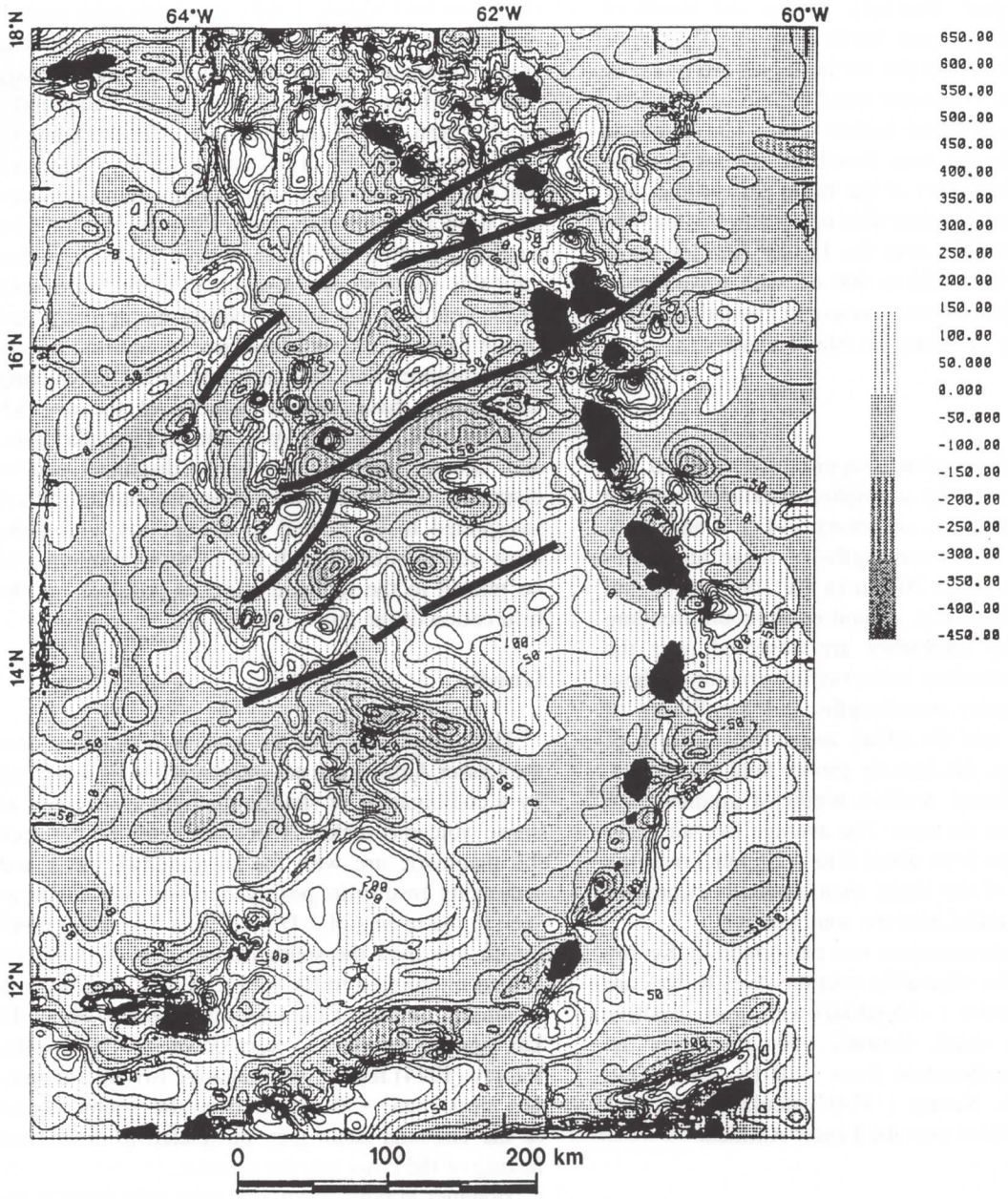

Fig. 9. Total intensity magnetic anomalies over the study area. Heavy solid and dashed lines indicate interpreted curvilinear zones of disruption (dashed lines indicate reduced confidence). Contour interval is 50 nT.

density of 2.0 or 2.67 g/cm^3 in the Bouguer calculation are the amplitudes of the resultant anomalies. Anomaly shapes and wavelengths are essentially unaffected by the calculations.

The large Bouguer gravity high over the center of the basin is interpreted to be caused by crustal thinning and the formation of the Grenada basin. This gravity high migrates southward as the rock density which replaces the water layer is increased, because as the water column increases, the increased density assigned to it produces increased anomaly amplitudes. Small wavelength anomalies over the Lesser Antilles and Aves Ridge are relatively unchanged by the calculation. If the Bouguer gravity is compensating for the effect of the water bottom, then cross-cutting northeast-trending discontinuities also seen in these maps are interpreted to be related to deep-seated, crustal features

Two-dimensional models

Two-dimensional models were constructed using profile gravity, bathymetry and seismic (both reflection and refraction) data. Basement horizons, interpreted from multiple channel seismic reflection lines, were converted to depth prior to being incorporated in models. Oceanic crustal layers 2 and 3, and a probable transition from lower crust to man-

Table 4
Densities used in 2-D and 3-D forward models

Layer	Density (g/cm^3)
2-D and 3-D	
Water	1.03
Sediments	2.30
Layer 2 (basement or upper crust)	2.57
2-D only	
Layer 3 (lower crust)	2.74
Transition	3.05
Mantle	3.30

tle velocity, were incorporated utilizing refraction information. Densities were interpolated from the Nafe–Drake curve (Ludwig et al., 1971). In order to maintain consistency throughout the study area, density variations were not introduced within individual rock layers of the models. Table 4 displays horizons and densities used in modeling.

Depth conversion of two-way seismic reflection time is achieved by utilizing a velocity function derived from velocity analyses of seismic line C1904 (LDGO). This velocity function is developed in a two-step process. First, the velocity analyses in the basin are converted to depth using the Dix formula (Dix, 1955). Time versus depth curves are then overlain and a 'best fit' curve is determined. Second, the interpreted velocity curve is modified to satisfy seismic refraction data. Reversed seismic refraction line 29 (Officer et al., 1957) indicates that the top of oceanic seismic layer 2 is at about 8 km below sea level near LDGO line 15, cruise RC1904. The lower limit of the velocity function was set at this point.

The use of a single velocity function for basinwide time-to-depth conversions is easily implemented, but there are inherent pitfalls. The sediment and water layer thicknesses vary from 0 to 9 km and 0 to 3 km, respectively. The effect of an average velocity function tends to make shallow horizons too deep, and deep horizons too shallow. A high degree of accuracy with respect to shallow depth conversions is not critical for the purpose of this study. Fortunately the velocity analyses from cruise RC1904 are tied to seismic refraction velocities, hence the accuracy of depth conversions for deep horizons is good (± 0.5 km) when considering the overall dimensions of the basin (640 by 140 km).

Connecting models (A–B, B–C, and C–D–E) over the Grenada basin, oriented north–south and concentric with the Lesser Antilles Arc, reveals that the depth to the base of oceanic crustal layer 3 (Ludwig et al., 1971) decreases from about 20 to 18 km in C–D–E and remains nearly constant at about 15 km thereafter (Fig. 11). The combined thickness of oceanic crustal layers 2 and 3 decreases from about 15 km in the south, to 8 km in the center of B–C (near 14.5°N), and then increases to 15 km to the north. In general, the thickness of the transitional layer is modeled to thicken away from the central portion of the basin. East–west-oriented models (F–F′ and G–G′) reveal that the minimum depth to the base of oceanic crustal layer 3 ranges from 13 to 15 km (Fig. 12). These minima are located at about 62.5°W and 61.5°W for models F–F′ and G–G′, respectively. The combined thickness of layers 2 and 3 ranges from about 17 km (Aves Ridge) to 7 km (Grenada basin) to 28 km (Lesser Antilles arc).

For the two-dimensional model F–F′, the depth to the base of layer 3 decreases to about 15 km at 15.75°N, 62.5°W and increases to about 17 km to the east (Fig. 12A). The minimum combined thickness of combined layers 2 and 3 is 11 km. Dramatic variations in the combined thickness of layers 2 and 3 modeled in the eastern part of F–F′ are interpreted to be related to the discontinuities. Other dramatic variations in the combined thickness of layers 2 and 3 are observed in the western part of F–F′. These variations are interpreted to represent density variations within the Aves Ridge. In model G–G′, the shape of the base of layer 3 is asymmetric and shallowest (about 14 km) in the eastern part of the model (14.25°N, 61.5°W). From here the depth increases east and west to about 18 km (Fig. 12B).

Overall, the two-dimensional models display good correlations between calculated gravity and free-air gravity profiles. Long-wavelength gravity anomalies over this area are considered to be two-dimensional because of the overall north–south trough-like shape of the gravity field over the study area. The excellent correlation of gravity profiles adds confidence to the overall concept of the basin's crustal structure. That is, the crust of the Grenada basin thins toward the center and thickens under the Aves Ridge and Lesser Antilles island arc. The observed gravity data are consistent with such a model.

Three-dimensional models

A three-dimensional forward model was constructed to help interpret gridded gravity data. Gridded bathymetry data and an interpreted depth to acoustic basement surface (Speed and Westbrook, 1984) were incorporated into a two-and-one-half layer model representing the water column, sediments, and basement respectively. The depth to acoustic basement surface was interpreted from two-way travel time using many of the multi-channel seismic lines utilized in this study (Speed and Westbrook, 1984). Fig. 13, and Web-Figs. 15.9,10, show the depth-to-acoustic basement surface used in 3-D

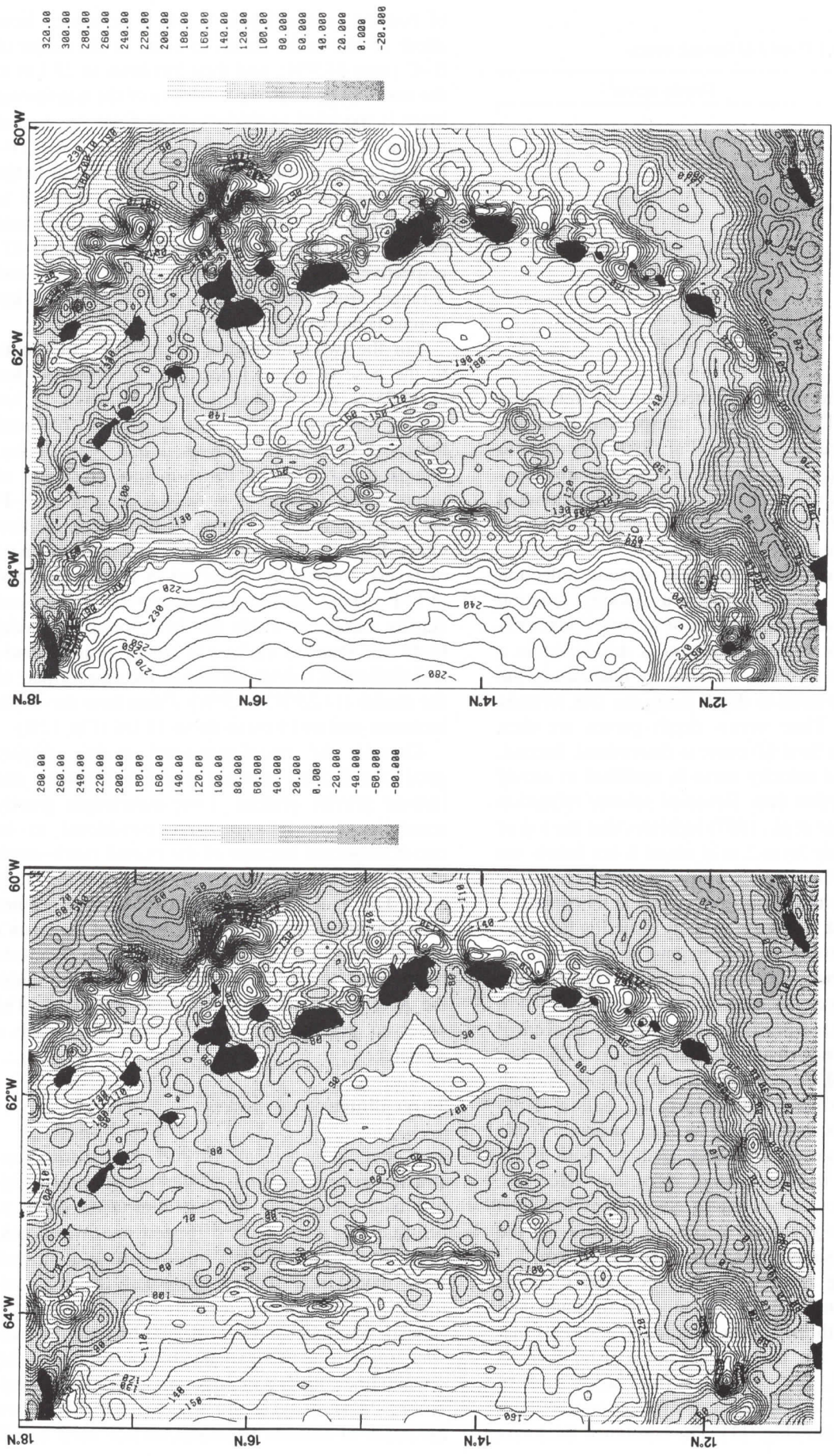

Fig. 10. Bouguer gravity anomalies over the study area calculated by substituting rock density of (A) 2.0 g/cm^3 and (B) 2.67 g/cm^3 for the water layer. Contour interval is 10 mGal.

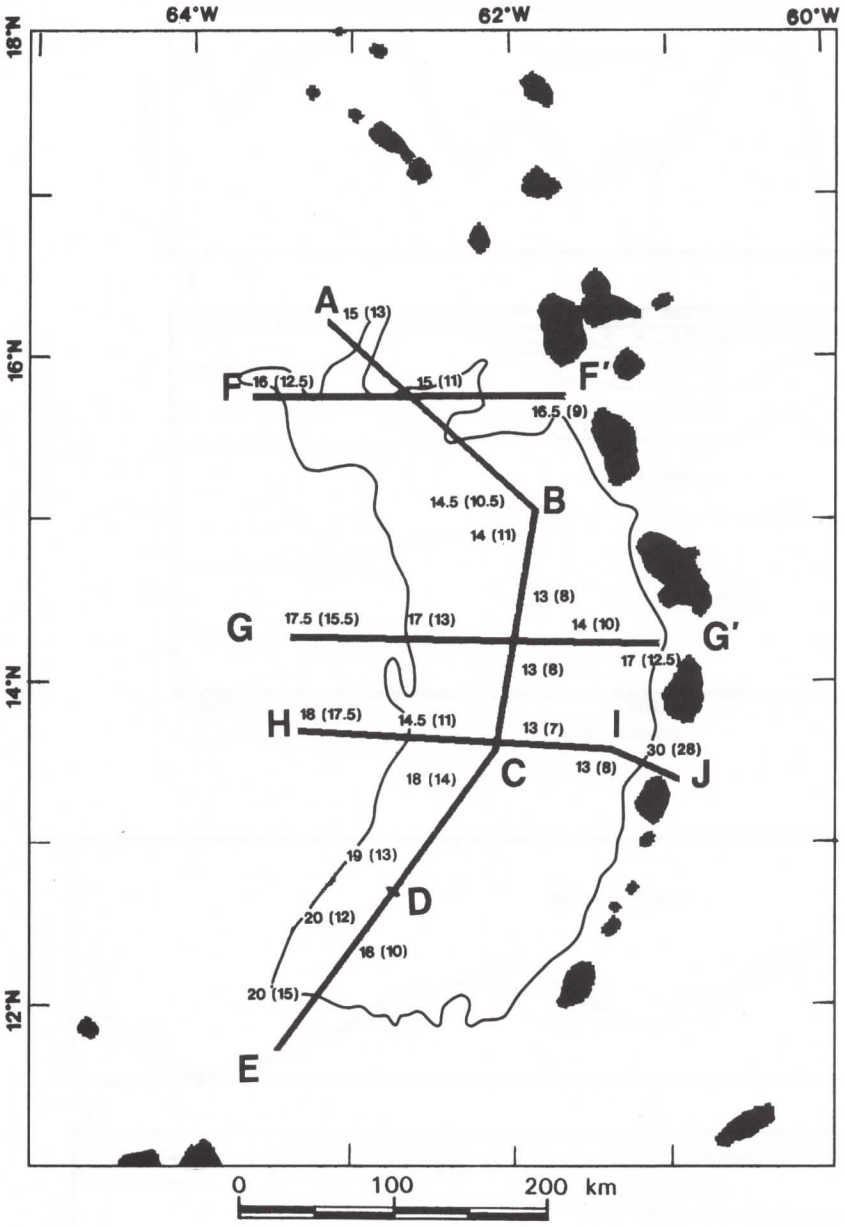

Fig. 11. Locations for 2-D models of the basin. Posted values coincide with depth (km) to the base of layer 3 (Ludwig et al., 1971) and combined thickness (in parentheses) of both layers 2 and 3 from results of 2-D forward modeling.

modeling. Speed and Westbrook (1984) interpreted this basement surface in time (Web-Fig. 15.11) utilizing extensive multiple- and single-channel seismic reflection data sets. This surface was converted to depth utilizing the velocity function described above.

The calculated gravity field is produced by the water layer, sediment layer, and the upper surface of layer 2. The observed free-air gravity field is produced by these same layers as well as layer 3, the transitional layer, and deeper sources. The observed free-air gravity field also reflects density variations within the sediments and basement which are unknown, as well as variations in crustal thickness. In general, density variations within the sediments and shallow parts of the basement should produce short-wavelength anomalies. With respect to long-wavelength anomalies, the calculated gravity field (Fig. 14A and Web-Fig. 15.12) correlates well with the observed free-air gravity field; however, there are several important differences between the calculated and observed fields. The location of the gravity minima over the Grenada basin is displaced to the north for the calculated field. A north–south-trending, subtle, broad high is superimposed along the center of the basin for the observed free-air gravity. The area of the continental shelf of Venezuela exhibits an anomaly high in the calculated gravity. The observed free-air gravity field has high frequency anomalies, particularly over the Aves Ridge and Lesser Antilles, which are not observed in the calculated field.

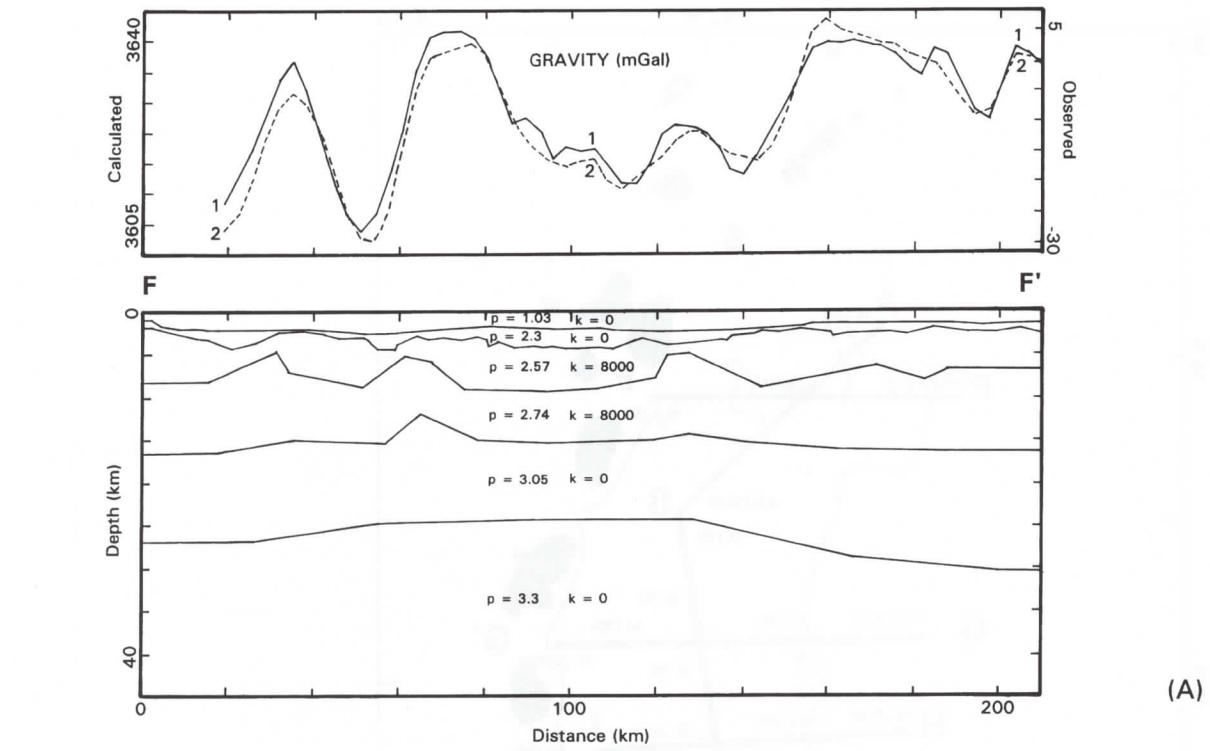

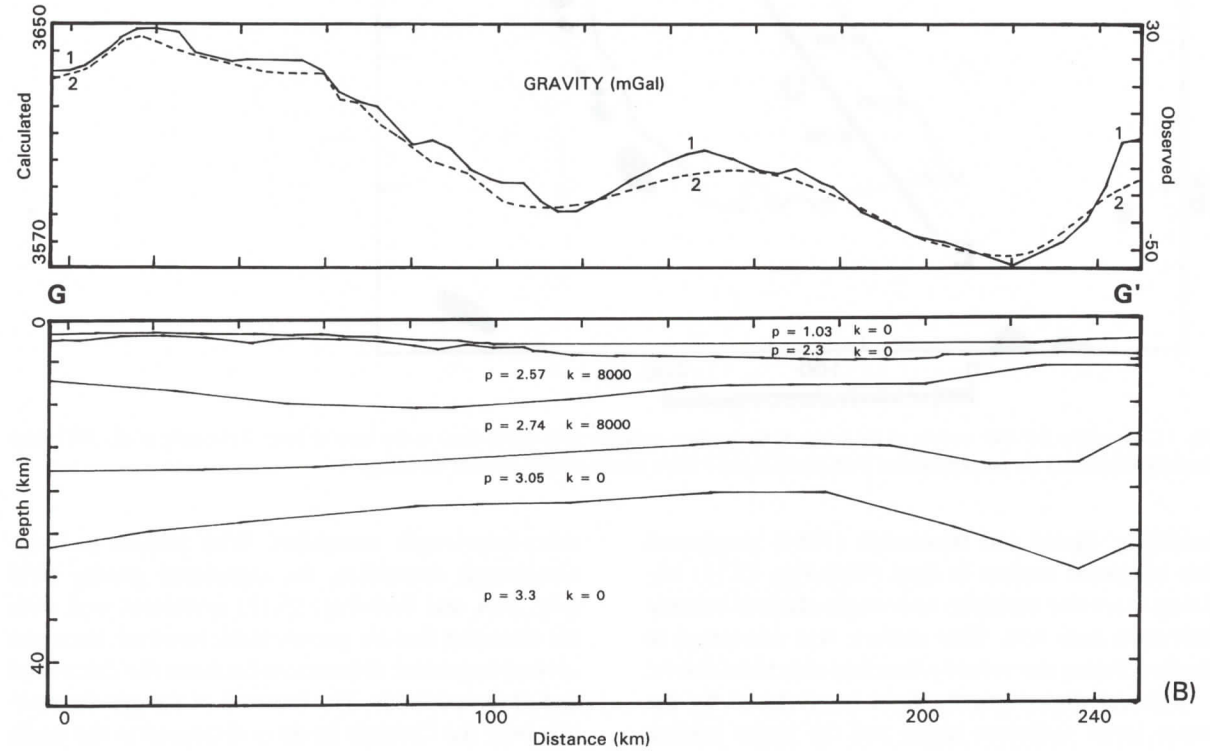

Fig. 12. (A) 2-D model F–F′ oriented east–west in the northern part of the basin. (B) 2-D model G–G′ oriented east–west in the central part of the basin. Horizontal and vertical scales of the models are 1 : 1.5 and 1 : 0.75 million (2 : 1 vertical exaggeration); *1* = observed gravity (free-air) profile; *2* = calculated gravity profile.

To increase confidence in the 3-D model, the free-air gravity field is filtered (high cut: 60 km) to remove short-wavelength anomalies, then the calculated gravity is subtracted from the filtered free-air gravity (Web-Figs. 15.13,14). This operation isolates anomalies which are produced by deep crustal and upper mantle variations. Residual gravity anomalies over the basin are similar to Bouguer gravity anoma-

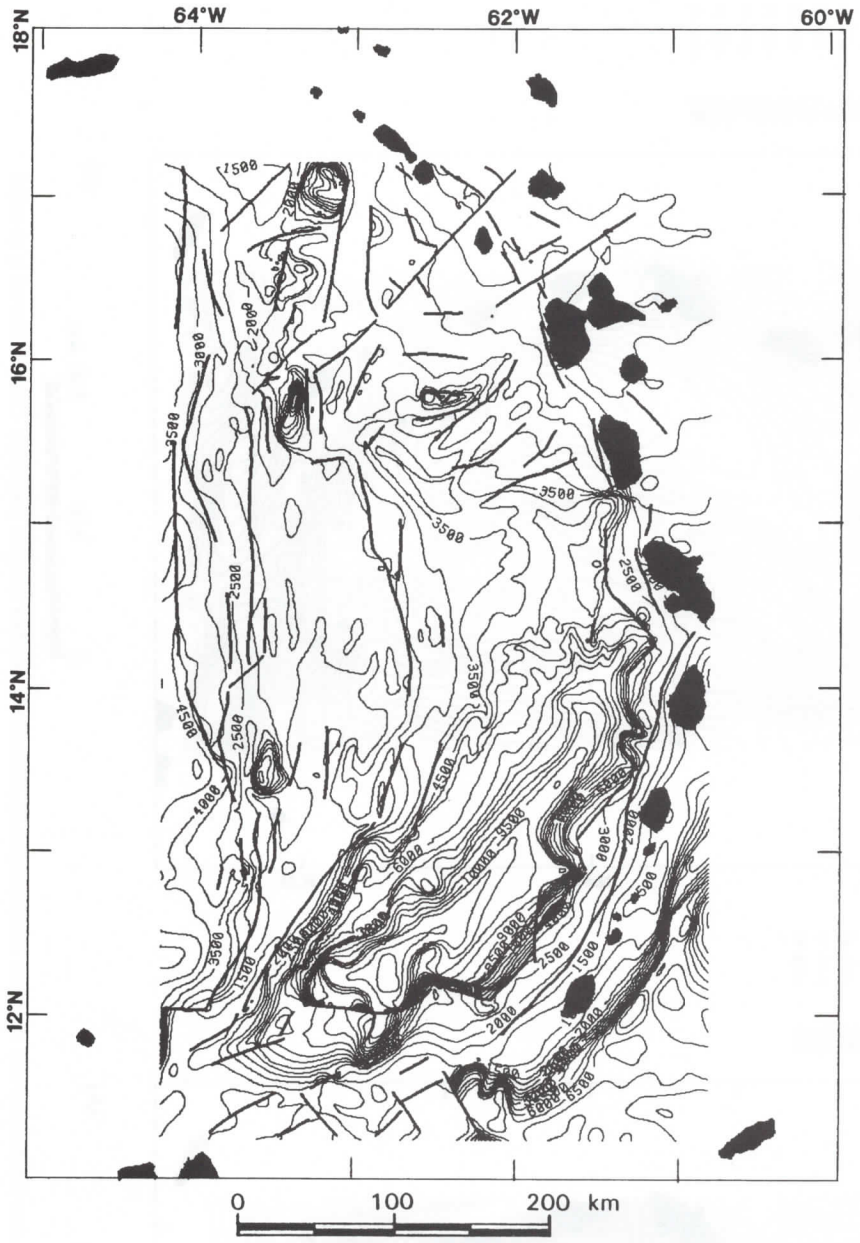

Fig. 13. Depth to acoustic basement with heavy lines indicating faults (after Speed and Westbrook, 1984). Contour interval is 500 m.

lies and are defined here as residual Bouguer anomalies. A broad high exists over the basin and lows over the Aves Ridge and Lesser Antilles arc. Also, the triangular-shaped anomaly over the southernmost part of the basin correlates well with Bouguer anomalies.

DISCUSSION

A key to understanding the Grenada basin is an understanding of the differences and similarities between the northern and southern parts of the basin. The differences are dramatic for bathymetry, seismic reflection, and magnetic data. However, free-air and Bouguer gravity data suggest that the crustal structure of the basin is broadly similar from north to south. Although seismic refraction coverage is sparse in the north, when utilized as control for two-dimensional and three-dimensional modeling, these data also indicate similarities from north to south.

The only mantle velocity (8.2 km/s) recorded for the basin is Lesser Antilles Seismic Project (LASP) Profile B (Boynton et al., 1979) and is oriented approximately east–west near 13°N (Fig. 15). Two-D model G–G′ is crossed by the north-northeast-oriented reversed Profile 29 (Ewing et al., 1957). There is no doubt that the crust in this part of the basin is similar to typical oceanic layering. Average velocities of back-arc basins are 5.1, 6.4, 7.3, and 8.2 km/s for layer 2, layer 3, transition, and mantle,

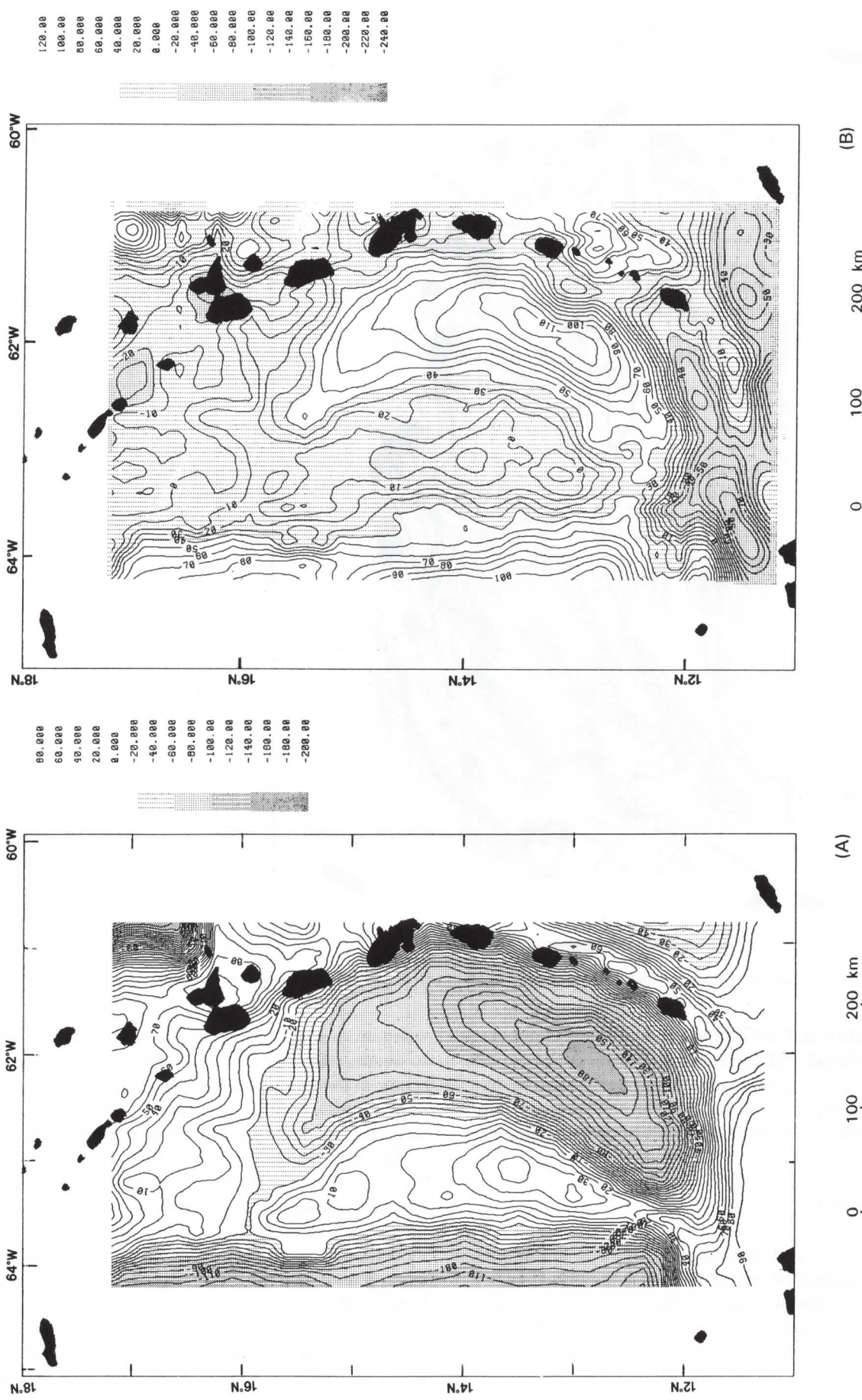

Fig. 14. (A) Calculated gravity anomalies (free-air) over the study area. (B) Filtered free-air minus calculated gravity anomalies = residual Bouguer anomalies. Contour interval is 10 mGal.

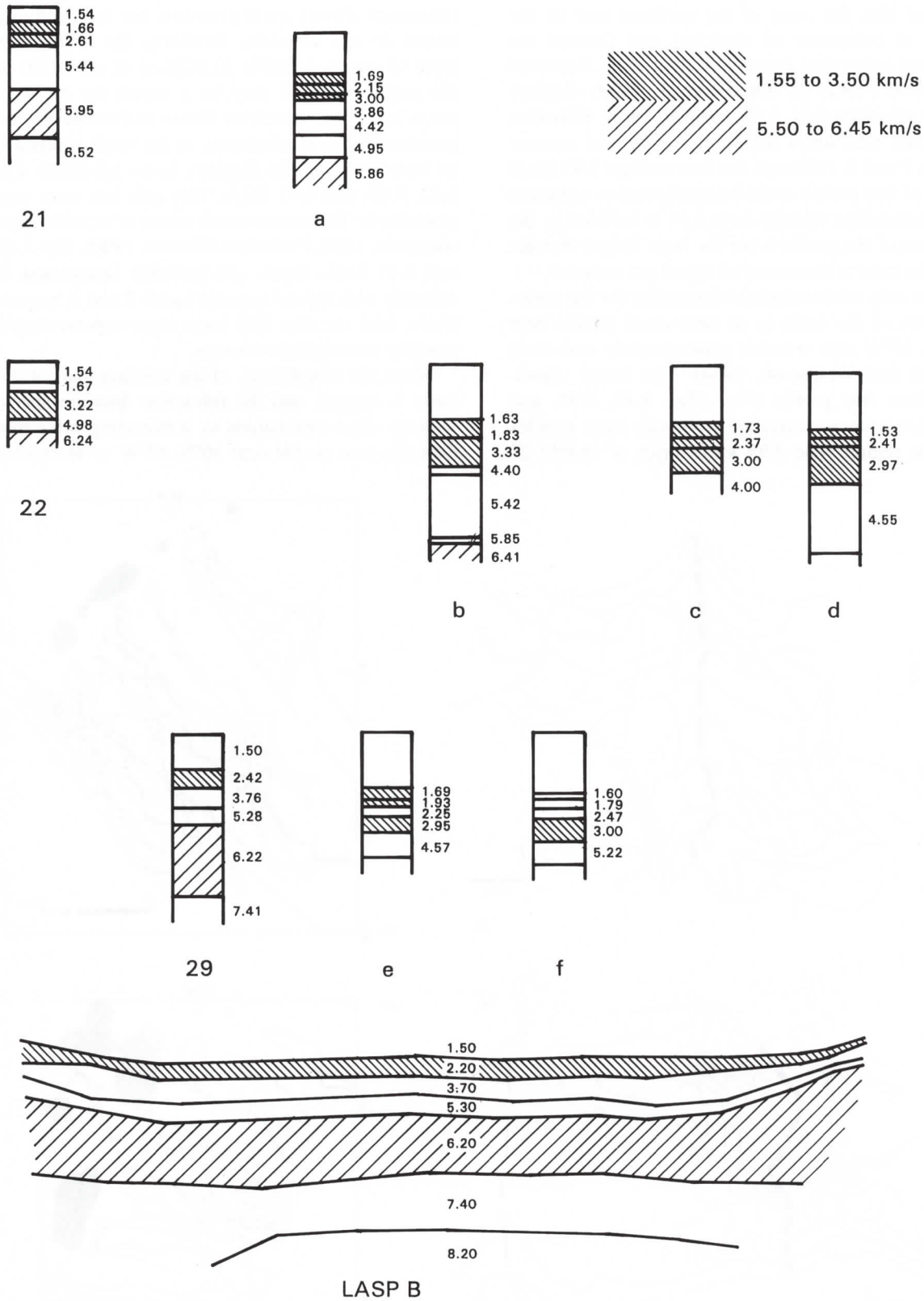

Fig. 15. Refraction velocities in the Grenada basin. Locations of velocity profiles are shown in Fig. 7B.

respectively (Table 3). Similarly, lower velocities for profiles LASP B and 29 are 5.30, 6.20, 7.40, 8.2 km/s and 5.28, 6.22, 7.41 km/s, respectively. Velocities 5.28 or 5.30 and 6.22 or 6.30 km/s correlate with typical oceanic crustal layers 2 (5 km/s) and 3 (6.4 to 7.1 km/s) described by Ludwig et al. (1971).

In their models for the formation of the Grenada basin, Bouysse (1988) and Pindell and Barrett (1990)

suggest that the crust of the northern part of the basin is composed of stretched and thinned arc material rather than accreted oceanic crust. Reversed refraction Profile 21 (Officer et al., 1959) displays lower velocities 5.44, 5.95, and 6.52 km/s. Velocities 5.44 and 6.52 km/s are similar to typical oceanic layers 2 and 3. Although the intermediate 5.95 km/s layer of this profile could be interpreted to represent an intermediate velocity from 5.44 to 6.52 km/s, the location of the profile (over the Aves Ridge) dictates that the crust is composed of island arc material.

The only other velocity information for the northern part of the basin is an unreversed profile near 16°N, 63°W and oriented approximately east–west (Speed and Westbrook, 1984). The lower velocities from this profile (Fig. 15a), 4.42, 4.95, and 5.86 km/s do not correlate well with other profiles for the region. The 5.95 km/s layer of Profile 21 (discussed above) could correlate, but the overlying layers do not correlate. Similarly, the 4.98 km/s layer of reversed Profile 22 (Officer et al., 1959) to the south-southwest may be a match for the 4.95 km/s layer, but velocities above and below do not correlate either. Furthermore, to the south-southeast, an unreversed profile displays lower velocities 4.4, 5.42, 5.85, and 6.41 km/s. This area has been suggested to be the northernmost extent of oceanic crust (Bouysse, 1988; Pindell and Barrett, 1990). The 5.42 and 6.41 km/s layers are probably interpreted to coincide with typical oceanic layers 2 and 3, respectively, with the thin 5.85 km/s layer representing a possible intermediate velocity.

Since the morphology of the northern part of the basin is rugged, and the refraction data are sparse with no clear correlations to surrounding refraction data, the lone profile near 16°N, 63°W is interpreted

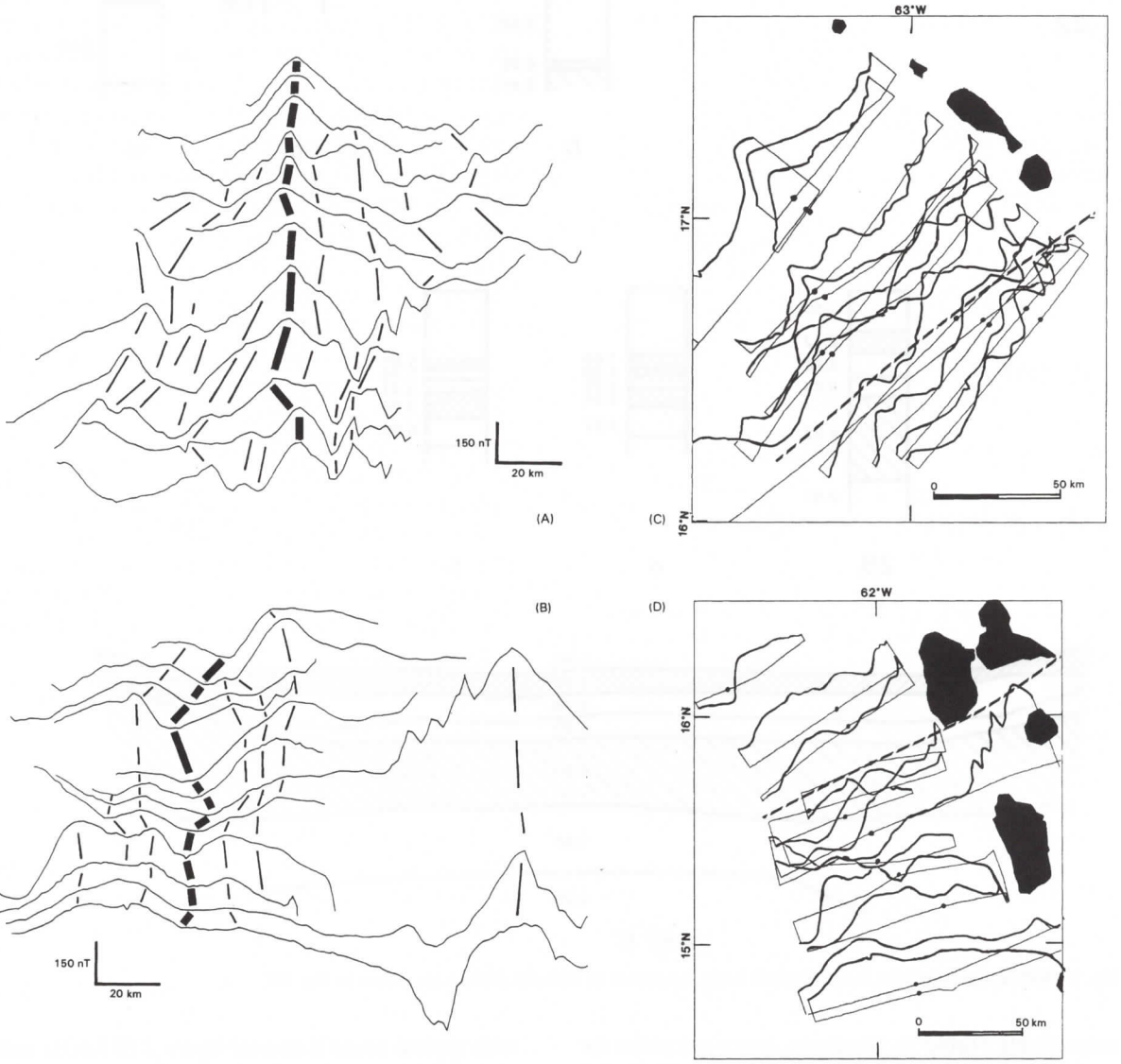

Fig. 16. Magnetic anomaly profiles: (A, C) correlated; (B, D) displayed in their acquisition position. Heavy lines in (A) and (B) indicate correlated anomalies. Dots in (B) and (D) correspond to locations of correlated anomalies in (A) and (B). Dashed lines correspond to interpreted curvilinear zones of disruption (Fig. 3).

to be less reliable than the rest of the refraction information. Therefore, the nature of the crust for the northern part of the basin remains relatively uncertain. Two-dimensional and three-dimensional gravity models suggest that crustal layers gradually thin to the north in this region. The Bouguer gravity over the Grenada basin has been calculated four times using two methods in this work as well as twice by Kearey (1974; Kearey et al., 1975). Anomaly patterns produced by all these calculations are similar. The resultant long-wavelength high over the central part of the basin diminishes gradually north to the Saba Bank, and south to the continental slope of Venezuela. This indicates that the thickness of the crust of the basin also changes gradually over the length of the basin.

In his discussion regarding the magnetic anomalies over the Grenada basin, Bouysse (1988) points out that, "... the present great depth to the oceanic basement due to sedimentary overloading combined with a possible location of the Eastern Caribbean in the vicinity of the geomagnetic equator during the Paleocene may contribute to significantly lowering the anomalies' intensity and to blur the original pattern." Although the geophysical data in the Grenada basin are complex, our interpretation suggests that the formation of the Grenada basin was by near east–west extension. And though the nature of the crust of the northern part of the basin cannot be determined conclusively, a mechanism for which oceanic crust was later disrupted by tectonism related to the bifurcation of the Lesser Antilles arc is suggested.

Strike-slip motion (Speed and Westbrook, 1984) along prominent east-northeast faults in the northern part of the basin may have caused the magnetic signature over this part of the basin to be disrupted. McCann and Sykes (1984) identified magnetic anomalies having amplitudes of over 400 nT produced by fracture zones in oceanic crust, during the Cretaceous quiet period, just north of Hispaniola and Puerto Rico. In order to test this hypothesis, magnetics profiles were re-interpreted with the specific purpose to identify, and correlate displaced anomalies, or packages of anomalies. Fig. 16A,C displays correlated anomaly profiles over the basin and Fig. 16B,D shows the same profiles plotted in their acquisition position. For Fig. 16A,B the northern six profiles may be displaced about 45 km to the southwest with respect to the southern five profiles over this area. The central high (dots) is shown in both figures. Fig. 16C,D is a somewhat less convincing correlation. For this set of profiles, dots follow

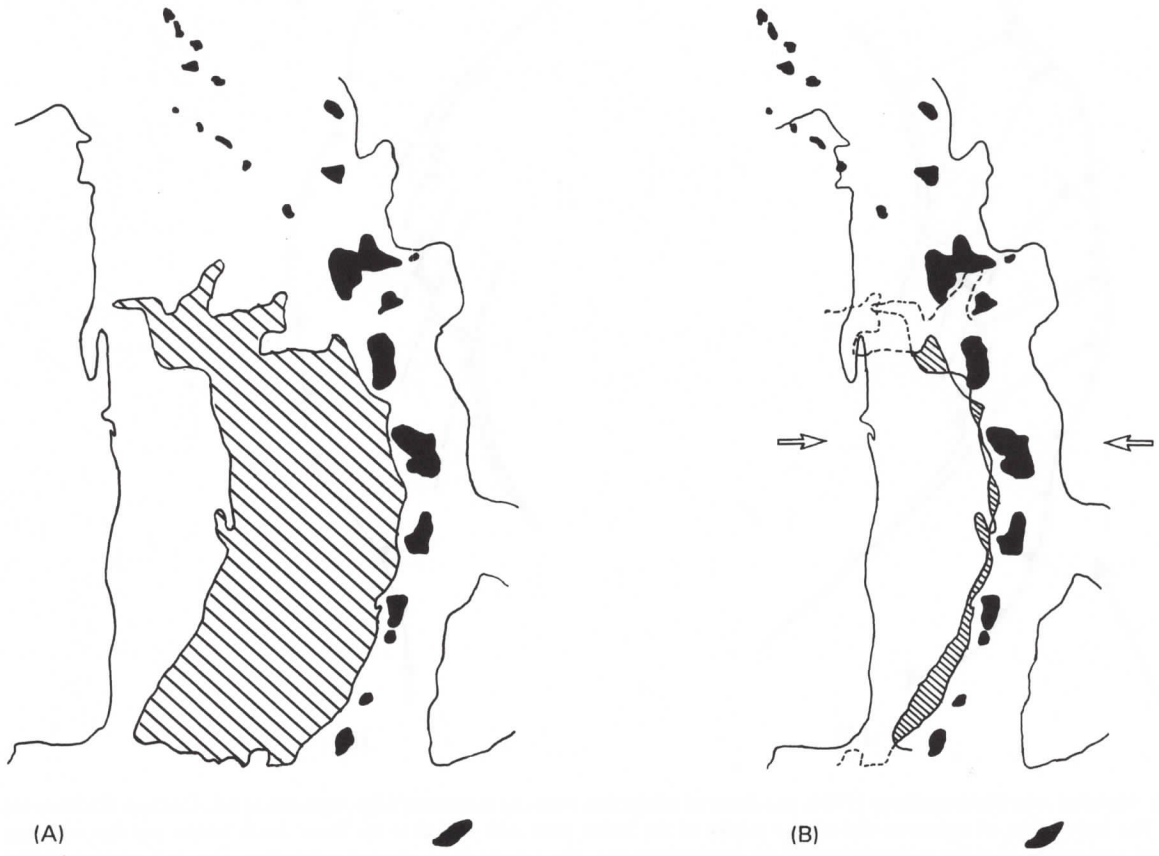

Fig. 17. East–west reconstruction of the Grenada basin using 2 km isobath: (A) present-day configuration; (B) east–west closure of the basin.

the correlated prominent low. These anomalies may be displaced about 25 km.

Fig. 17 shows a simple east–west closing of the Grenada basin along the 2 km isobath. Although the fit is generally good, the basin does not close completely in the south and the isobaths overlap in the north. Knowledge of seafloor spreading geometries and the amount of extension of the arc prior to spreading would allow a better constrained reconstruction. Furthermore, the poor fit in the north is consistent with our interpretation that the island arc has been tectonically modified since the formation of the basin.

There are two important aspects of the north–south (Pindell and Barrett, 1990) and northeast–southwest (Bouysse, 1988) spreading models suggested for the formation of the Grenada basin. There is no real world analogy for these suggested mechanisms. Although Brooks et al. (1984) have classified the Sulu and Celebes Sea basins as possibly being back-arc basins with the westward dipping Philippine plate related to extension, these basins are probably trapped, small ocean basins (McCabe et al., 1985, 1986; Lee and McCabe, 1986; McCabe and Cole, 1987). The only other back-arc basin in the world which exhibits extension oblique to the trench line of the subduction zone is the Andaman Sea basin. However, there is no counterpart for the Aves Ridge here. That is, a remnant island arc is not bounded by basins on both sides. If oblique subduction resulted in oblique back-arc extension and formation of the Grenada basin, then it is reasonable that the Aves Ridge would be composed of oblique-oriented segmented arc sections.

Fig. 18A shows a trace of the subduction zone and ridge/transform sections in the Andaman Sea

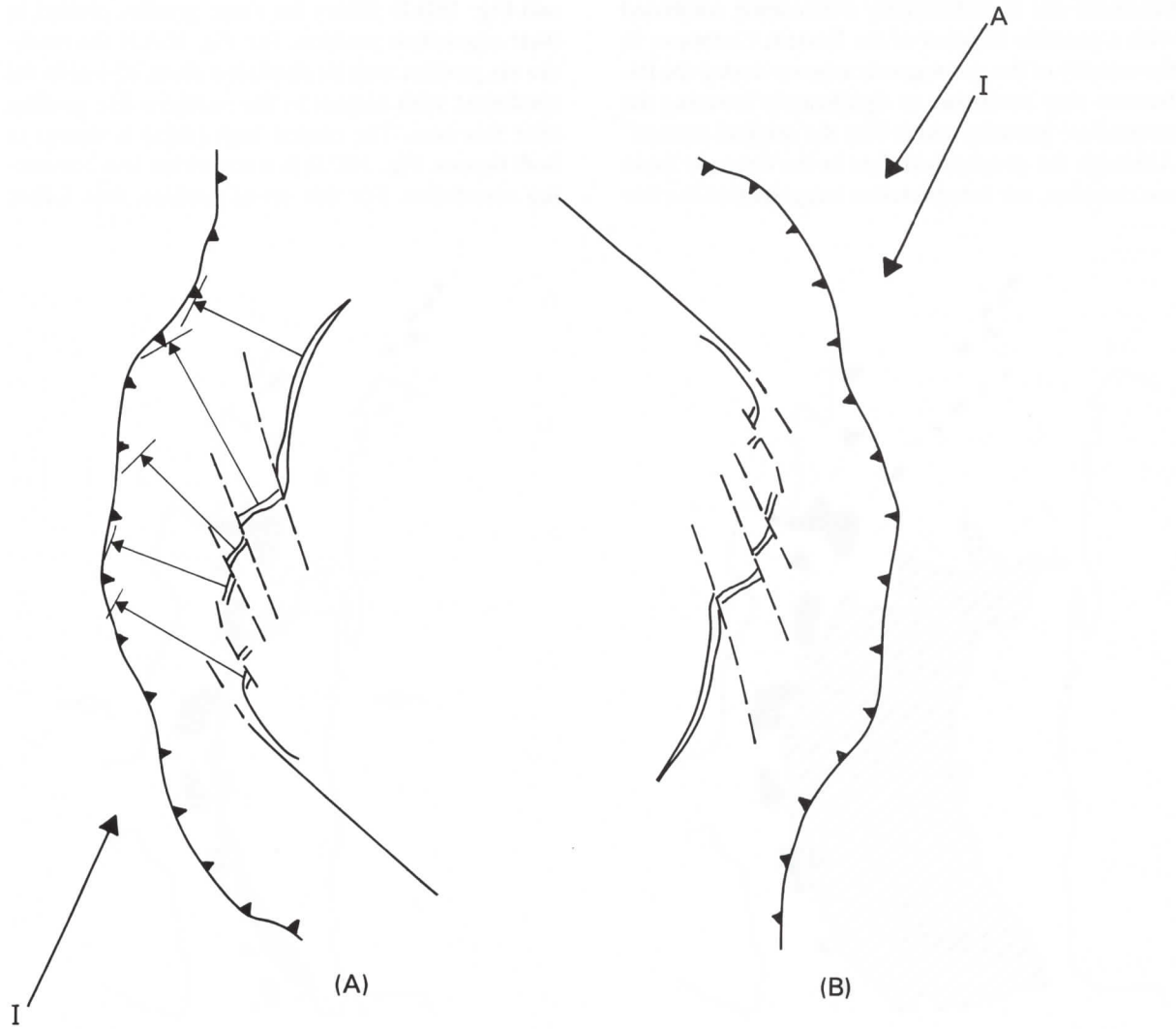

Fig. 18. Modified after Mukhopadhyay (1984). (A) Trace of subduction zone and transform/ridge segments in the Andaman Sea back-arc basin. The large vector (*I*) represents the relative motion of the Indian plate with respect to the basin. Small arrows and line segments represent projections of ridge segments toward the subduction zone. (B) Upside-down trace of subduction zone and transform/ridge segments in the Andaman Sea back-arc basin. The large vector (*A*) represents the relative motion between the North/South American plates and the Lesser Antilles subduction zone included for comparison of Andaman Sea and Grenada Basins.

(after Mukhopadhyay, 1984). The large vector (I) in Fig. 18A represents the direction of motion of the Indian plate with respect to the island arc. Oblique to the arc back spreading is apparent; however, if one projects individual ridge segments back to the subduction zone perpendicular to ridge segments (small arrows and connecting segments), then these segments are subparallel to the arc for the most part. In Fig. 18B the previous trace of the Andaman Sea is turned upside down. The second vector (A) represents suggested oblique subduction for the Atlantic plate and the Lesser Antilles (Pindell and Barrett, 1990). The similarity between the Andaman Sea and Grenada basins is obvious. Furthermore, the ridge/transform pattern is similar to the tectonic model for the evolution of the Grenada basin (Fig. 6) and the pattern predicted by Dewey (1980) regarding the mechanism for back-arc spreading.

There are at least nineteen basins which have formed via back-arc extension in the world today. All but possibly two of these basins exhibit extension perpendicular to the subduction zone. Therefore, with the physiography of the study area in mind, near east–west extension for the formation of the Grenada basin is favored. Second, it is felt that conditions which cause back-arc spreading are primarily a result of the interaction between the subducting slab and the overriding plate. Both north–south (Pindell and Barrett, 1990) and northeast–southwest (Bouysse, 1988) spreading models for the formation of the basin rely on coupling along the Caribbean/South American plate transform boundary for back-arc extension. In the Southwest Pacific, the Fiji Plateau, South Fiji basin, and Lau basin are back-arc regions which have formed juxtaposed to transform faults. Magnetic lineations over the Fiji Plateau are oriented subparallel to the subduction zone (Brooks et al., 1984). Extension in the South Fiji basin is from a ridge–ridge–ridge triple junction (Weissel, 1981). The spreading ridge of the Lau basin is parallel to the Tonga Trench (Taylor and Karner, 1983) and forms a small transform–ridge–transform triple junction near the bounding transform fault to the north. These back-arc regions have not formed as predicted by the trench transform model. Hence, the coupling along a transform fault may only have a minor influence on the development of back-arc basins.

CONCLUSION

Thorough analyses of magnetic, gravity and seismic data support near east–west extension for the formation of the Grenada basin. Interpretation of magnetic data included trend analyses and forward modeling (Bird et al., 1993). We have integrated these results with analyses of gravity and seismic data to develop a more coherent model for the evolution of the Grenada basin. This evolution involves two major tectonic episodes. The basin is interpreted to have formed by near east–west back arc seafloor spreading in early Tertiary time. In late Tertiary time, the northern part of the basin was affected by compressional forces causing the Lesser Antilles island arc to split, displacing a section of the Aves Ridge, and disrupting the crust of Grenada basin, including its magnetic signature.

REFERENCES

Bandy, W.L. and Hilde, T.W.C., 1983. Structural features of the Bonin Arc: implications for its tectonic history. Tectonophysics, 99: 331–353.

Barker, P. and Hill, I.A., 1981. Back-arc extension in the Scotia Sea. Philos. Trans. R. Soc. London, A300: 249–262.

Bibee, L.D., Shor, G.G. and Lu, R.S., 1980. Inter-arc spreading in the Mariana Trough. Mar. Geol., 35: 183–197.

Bird, D.E., 1991. An Integrated Geophysical Interpretation of Grenada Basin. M.S. Thesis, Univ. of Houston, 316 pp.

Bird, D.E., Hall, S.A., Casey, J.F. and Millegan, P.S., 1993. Interpretation of magnetic anomalies over the Grenada Basin. Tectonics 12 (5): 1267–1279.

Bougault, H., Dmitriev, L., Schilling, J.G., Sobolev, A., Joran, J.L. and Needham, H.D., 1988. Mantle heterogeneity from trace elements: MAR triple junction near 14°N. Earth Planet. Sci. Lett., 88: 27–36.

Bouysse, P., 1984. The Lesser Antilles arc: structure and geodynamic evolution. Init. Rep. DSDP, 78A: 83–103.

Bouysse, P., 1988. Opening of the Grenada back-arc basin and evolution of the Caribbean plate during the Mesozoic and Early Paleocene. Tectonophysics, 149: 121–143.

Boynton, C.H., Westbrook, G.K., Bott, M.H.P. and Long, R.E., 1979. A seismic refraction investigation of crustal structure beneath the Lesser Antilles island arc. Geophys. J. R. Astron. Soc., 58: 371–393.

Brooks, D.A., Carlson, R.L., Harry, D.L., Melia, P.J., Moore, R.P., Rayhorn, J.E. and Tubb, S.G., 1984. Characteristics of back-arc regions. Tectonophysics, 102: 1–16.

Clark, T.F., Korgen, B.J. and Best, D.M., 1978. Heat flow in the eastern Caribbean. J. Geophys. Res., 83: 5883–5891.

Cross, T.A. and Pilger, R.H., Jr., 1982. Controls of subduction geometry, location of magmatic arcs, and tectonics of arc and back-arc regions. Geol. Soc. Am. Bull., 93: 545–562.

Curray, J.R., Moore, D.G., Lawver, L.A., Emmel, F.J., Raitt, R.W., Henry, M. and Kieckhefer, R., 1979. Tectonics of the Andaman Sea and Burma: In: J.S. Watkins, L. Montadert and P.W. Dickerson (Editors), Geological and Geophysical Investigation of Continental Margins. Am. Assoc. Pet. Geol., pp. 189–198.

Dewey, J.F., 1980. Episodicity, sequence, and style at convergent plate boundaries. In: D.W. Strangway (Editor), The Continental Crust and its Mineral Deposits. Geol. Assoc. Can., Spec. Pap., 20: 553–573.

Dix, C.H., 1955. Seismic velocities from surface measurements. Geophysics, 20: 68–86.

Duncan, R.A. and Hargraves, R.B., 1984. Plate tectonic evolution of the Caribbean region in the mantle reference frame. In: W.E. Bonini, R.B. Hargraves and R. Shagan (Editors), The Caribbean–South American Plate Boundary and Region Tectonics. Geol. Soc. Am. Mem., 62: 81–93.

Edgar, N.T., 1968. Seismic Refraction and Reflection in the Caribbean Sea. Ph.D. Thesis, University of Columbia.

Ewing, J.I., Officer, C.B., Johnson, H.R. and Edwards, R.S., 1957. Geophysical investigations in the eastern Caribbean: Trinidad Shelf, Tobago Trough, Barbados Ridge, Atlantic Ocean. Bull. Geol. Soc. Am., 68: 897–912.

Fink, L.K., 1968. Marine Geology of the Guadeloupe Region, Lesser Antilles Arc. Ph.D. Dissertation, University of Miami, FL.

Fink, L.K., 1970. Field guide to the island of La Desirade with notes on the regional history and development of the Lesser Antilles island arc. Int. Field Inst. Guideb. to the Caribbean Island-Arc System, Am. Geol. Inst. N.S.P., pp. 287–302.

Fox, P.J. and Heezen, B.C., 1975. Geology of the Caribbean crust. In: A.E.M. Nairn and F.G. Stehli (Editors), The Ocean Basins and Margins. Plenum Press, London, 3, pp. 421–466.

Ghosh, N., Hall, S.A. and Casey, J.F., 1984. Seafloor spreading magnetic anomalies in the Venezuelan Basin. In: W.E. Bonini, R.B. Hargraves and R. Shagan (Editors), The Caribbean–South American Plate Boundary and Regional Tectonics. Geol. Soc. Am. Mem., 162: 65–80.

Hayes, D.E., Houtz, R.E., Jarrard, R.D., Mrozowski, C.L. and Watanabe, T., 1978. Crustal structure. In: D.E. Hayes (Editor), A Geophysical Atlas of East and Southeast Asian Seas. Geol. Soc. Am., Map Chart Ser., MC-25.

Hussong, D.M. and Uyeda, S., 1981. Tectonic processes and the history of the Mariana Arc: a synthesis of the results of deep sea drilling Leg 60. Init. Rep. DSDP, 60: 909–929.

Karig, D.E., 1971. Origin and development of marginal basins in the western Pacific. J. Geophys. Res., 76: 2542–2561.

Kearey, P., 1974. Gravity and seismic reflection investigations into the crustal structure of the Aves Ridge, eastern Caribbean. Geophys. J.R. Astron. Soc., 38: 435–448.

Kearey, P., Peter, G. and Westbrook, G.K., 1975. Geophysical maps of the eastern Caribbean. J. Geol. Soc. London, 131: 311–321.

Lee, C.S. and McCabe, R.J., 1986. The Banda–Celebes–Sulu Basin: a trapped piece of Cretaceous–Eocene oceanic crust? Nature, 322: 51–54.

Lee, C.S., Shor, G., Bibee, L.D., Lu, R.S. and Hilde, T.W.C., 1980. Okinawa Trough, origin of a back-arc basin. Mar. Geol., 35: 219–241.

Ludwig, W.J., Nafe, J.E. and Drake, C.L., 1971. Seismic refraction. In: A.E. Maxwell (Editor), The Sea, 1. John Wiley, New York, 4, pp. 53–84.

McCabe, R.J. and Cole, J.T., 1987. Speculations on the Late Mesozoic and Cenozoic evolution of the southeast Asian margin. Trans. 4th Circum-Pacific Energy and Mineral Resources Conf., 4: 375–394.

McCabe, R.J., Lee, C.S. and Hilde, T.W.C., 1985. The Sulu–Celebes–Banda basin — a trapped piece of oceanic crust (abstr.). Eos, 66: 1078.

McCabe, R.J., Hilde, T.W.C., Cole, J.T., Sager, W. and Lee, C.S., 1986. Sulu–Celebes–Banda Basins: a trapped piece of Cretaceous to Eocene oceanic crust (abstr.). Bull. Am. Assoc. Pet. Geol., 70: 930.

McCann, W.R. and Sykes, L.R., 1984. Subduction of aseismic ridges beneath the Caribbean Plate: implications for the tectonic and seismic potential of the northeastern Caribbean. J. Geophys. Res., 89: 4493–4519.

Mukhopadhyay, M., 1984. Seismotectonics of subduction and back-arc rifting under the Andaman Sea. Tectonophysics, 108: 229–239.

Officer, C.B., Ewing, J.I., Edwards, R.S. and Johnson, H.R., 1957. Geophysical investigations in the eastern Caribbean: Venezuelan Basin, Antilles Island Arc, and Puerto Rico Trench. Bull. Geol. Soc. Am., 68: 359–378.

Officer, C.B., Ewing, J.I., Hennion, J.F., Harkrider, D.G. and Miller, D.E., 1959. Geophysical investigations in the eastern Caribbean: summary of 1955 and 1956 cruises. Phys. Chem. Earth, 3: 17–109.

Okuma, S., Nakatsuka, T., Makino, M. and Morijini, R., 1990. Aeromagnetic constraints on the basement structure of the Okinawa Trough and East China Sea Basin (abstr.). Soc. Explor. Geophys. Expanded Abstr. Biogr., 1: 594–597.

Pindell, J.L. and Barrett, S.F., 1990. Geological evolution of the Caribbean region; a plate tectonic perspective. In: G. Dengo and J.E. Case (Editors), The Caribbean Region. Geol. Soc. N. Am., H, pp. 405–432

Pindell, J.L., Cande, S.C., Pitman III, W.C., Rowley, D.B., Dewey, J.F., LaBrecque, J. and Haxby, W., 1988. A plate-kinematic framework for models of Caribbean evolution. Tectonophysics, 155: 121–138.

Poehls, K.A., 1978. Intra-arc basins: a kinematic model. Geophys. Res. Lett., 5: 325–328.

Ross, M.I. and Scotese, C.R., 1988. A hierarchical tectonic model of the Gulf of Mexico and Caribbean region. Tectonophysics, 155: 139–168.

Sleep, N.H. and Toskoz, M.N., 1971. Evolution of marginal basins. Nature, 233: 548–550.

Speed, R.C., Westbrook, G.K., et al., 1984. Lesser Antilles arc and adjacent terranes. Atlas 10, Ocean Margin Drilling Program, Regional Atlas Series, Marine Science International, Woods Hole, Mass., 27 sheets.

Tamaki, K., 1985. Two modes of back-arc spreading. Geology, 13: 475–478.

Taylor, B., 1979. Bismark Sea: evolution of a back-arc basin. Geology, 7: 171–174.

Taylor, B. and Karner, G.D., 1983. On the evolution of marginal basins. Rev. Geophys., 21: 1727–1741.

Tomblin, J.F., 1975. The Lesser Antilles and Aves ridge. In: A.E.M. Nairn and F.G. Stehli (Editors), The Ocean Basins and Margins, Plenum Press, London, 3, pp. 467–500.

Uyeda, S. and Kanamori, H., 1979. Back-arc opening and the mode of subduction. J. Geophys. Res., 84: 1049–1061.

Warner, A.J., Jr., 1991. The Cretaceous age sediments of the Saba Bank and their petroleum potential. Trans. 12th Caribbean Geol. Conf., St. Croix, U.S.V.I., Miami Geological Society.

Weissel, J.K., 1980. Evolution of the Lau Basin by the growth of small plates. In: M. Talwani and W.C. Pittman III (Editors), Island Arcs, Deep Sea Trenches, and Back-arc Basins. Maurice Ewing Ser., Am. Geophys. Union, 1: 429–436.

Weissel, J.K., 1981. Magnetic lineations in marginal basins of the west Pacific. Philos. Trans. R. Soc. London, A300: 223–247.

Westbrook, G.K., 1975. The structure of the crust and upper mantle in the region of Barbados and the Lesser Antilles. Geophys. J.R. Astron. Soc., 43: 201–242.